Report No. CG-D-59-77

(13)
B.S.

VENT SYSTEM AND LOADING CRITERIA FOR AVOIDING TANK OVERPRESSURIZATION

R. P. WILSON, JR.
P. K. PHANI RAJ

FINAL REPORT

SEPTEMBER 1977

Document is available to the public through the
National Technical Information Service,
Springfield, Virginia 22151

Prepared for

DEPARTMENT OF TRANSPORTATION
UNITED STATES COAST GUARD
Office of Research and Development
Washington, D.C. 20590

1. Report No. USCG D-59-77	2. Government Accession No.	3. Recipient's Catalog No.
4. Title and Subtitle Vent System and Loading Criteria For Avoiding Tank Overpressurization.		5. Report Date SEP 1977
		6. Performing Organization Code
7. Author(s) R. P. Wilson, Jr. P. K. Phani Raj		8. Performing Organization Report No.
9. Performing Organization Name and Address Arthur D. Little, Inc. 20 Acorn Park Cambridge, MA 02140		10. Work Unit No. (TRAIS) 3302.20.1.3
		11. Contract or Grant No. DOT-CG-42,357-A
12. Sponsoring Agency Name and Address U.S. Coast Guard (G-DSA/TP44) Department of Transportation 400 7th Street, S. W. Washington, D. C. 20590		13. Type of Report and Period Covered Final Report.
		14. Sponsoring Agency Code G-DSA-1/TP44
15. Supplementary Notes 87p. ADL-77396-3		

16. Abstract

The extent of cargo tank overpressure during transfer operations was analyzed, taking into account cargo properties, tank characteristics, loading rate, and vent system design. It was found that typical venting systems in use today have more than adequate capacity for gas venting, but inadequate capacity for liquid overfill. The margins of safety for gas venting appear to be about a factor of three in loading rate and a factor of ten in the effective length to diameter ratio of the vent system. Cargo volatility has a relatively small effect on the potential overpressure hazard. For the case of liquid overfill, the maximum permissible ratio of loading rate (cu-ft per sec) to vent cross sectional area (sq-ft) is 9 ft/sec. Many cargo transfer operations currently equal or exceed this value. Furthermore, tank failure would be expected less than one minute after the tank becomes liquid full.

208 850.

17. Key Words Overpressure　　Venting Cargo tank　　Vent system Tankers　　Vapor relief Chemical tankers　　Bulkhead Overfill	18. Distribution Statement Document is available to the public through the National Technical Information Service, Springfield, VA 22161.

19. Security Classif. (of this report) Unclassified	20. Security Classif. (of this page) Unclassified	21. No. of Pages 80	22. Price

Form DOT F 1700.7 (8-72)　　Reproduction of completed page authorized

NOTICE

This document is disseminated under the sponsorship of the U. S. Department of Transportation in the interest of information exchange. The United States Government assumes no liability for the contents or use thereof.

The United States Government does not endorse products or manufacturers. Trade or manufacturers' names appear herein solely because they are considered essential to the object of this report.
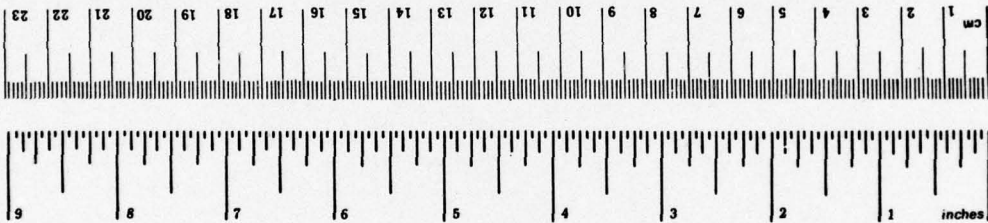
METRIC CONVERSION FACTORS

Approximate Conversions to Metric Measures

Symbol	When You Know	Multiply by	To Find	Symbol
		LENGTH		
in	inches	*2.5	centimeters	cm
ft	feet	30	centimeters	cm
yd	yards	0.9	meters	m
mi	miles	1.6	kilometers	km
		AREA		
in^2	square inches	6.5	square centimeters	cm^2
ft^2	square feet	0.09	square meters	m^2
yd^2	square yards	0.8	square meters	m^2
mi^2	square miles	2.6	square kilometers	km^2
	acres	0.4	hectares	ha
		MASS (weight)		
oz	ounces	28	grams	g
lb	pounds	0.45	kilograms	kg
	short tons (2000 lb)	0.9	tonnes	t
		VOLUME		
tsp	teaspoons	5	milliliters	ml
Tbsp	tablespoons	15	milliliters	ml
fl oz	fluid ounces	30	milliliters	ml
c	cups	0.24	liters	l
pt	pints	0.47	liters	l
qt	quarts	0.95	liters	l
gal	gallons	3.8	liters	l
ft^3	cubic feet	0.03	cubic meters	m^3
yd^3	cubic yards	0.76	cubic meters	m^3
		TEMPERATURE (exact)		
°F	Fahrenheit temperature	5/9 (after subtracting 32)	Celsius temperature	°C

*1 in = 2.54 (exactly). For other exact conversions and more detailed tables, see NBS Misc. Publ. 286, Units of Weights and Measures, Price $2.25, SD Catalog No. C13.10:286.

Approximate Conversions from Metric Measures

Symbol	When You Know	Multiply by	To Find	Symbol
		LENGTH		
mm	millimeters	0.04	inches	in
cm	centimeters	0.4	inches	in
m	meters	3.3	feet	ft
m	meters	1.1	yards	yd
km	kilometers	0.6	miles	mi
		AREA		
cm^2	square centimeters	0.16	square inches	in^2
m^2	square meters	1.2	square yards	yd^2
km^2	square kilometers	0.4	square miles	mi^2
ha	hectares (10,000 m^2)	2.5	acres	
		MASS (weight)		
g	grams	0.035	ounces	oz
kg	kilograms	2.2	pounds	lb
t	tonnes (1000 kg)	1.1	short tons	
		VOLUME		
ml	milliliters	0.03	fluid ounces	fl oz
l	liters	2.1	pints	pt
l	liters	1.06	quarts	qt
l	liters	0.26	gallons	gal
m^3	cubic meters	35	cubic feet	ft^3
m^3	cubic meters	1.3	cubic yards	yd^3
		TEMPERATURE (exact)		
°C	Celsius temperature	9/5 (then add 32)	Fahrenheit temperature	°F

°F -40   0   32   80   98.6   120   160   200   212
°C -40   -20   0   20   37   40   60   80   100

DOT-CG-42,357-A
ADL Reference 77396-3

VENT SYSTEM AND LOADING CRITERIA

FOR AVOIDING TANK OVERPRESSURIZATION

Prepared for:

Office of Research and Development
United States Coast Guard
400 Seventh Street, Southwest
Washington, D.C. 20590

June 1977

Arthur D. Little, Inc.
20 Acorn Park
Cambridge, MA 02140

Acknowledgements

The authors are indebted to Peter Athens and Bernard C. Hanley of Arthur D. Little, Inc. and Professor Robert Reid of the Massachusetts Institute of Technology for analyses of bulkhead structure and liquid cargo evaporation, respectively. Lieutenant Michael W. Taylor and Lieutenant Michael Flessner of the Marine Safety Branch, Division of Applied Technology, Office of Research and Development, United States Coast Guard provided helpful technical guidance to the authors during the performance of this work.

TABLE OF CONTENTS

I. BACKGROUND AND SUMMARY OF FINDINGS

Background

Venting systems are employed on marine vessels to relieve pressure differences which arise between the cargo tank and the ambient. Based on cargo flammability and toxicity, either of two types of venting systems is selected:

- ### Low Flammability and Toxicity

  Individual gooseneck vents fitted with flame screens and ball-check or pressure-relief valves: Here the pressure build-up during loading is negligible because open gauging is permitted.

- ### High Flammability or Toxicity

  Tanks manifolded to vent risers fitted with PV valves and/or flame arrestors: Here the normal pressure build-up during loading is 0 - 3 psig (depending on PV settings) because restricted or closed gauging is required.

In the latter case if the cargo pumping rate exceeds the vapor relief capacity, or if there is an accidental overfill, the pressure difference can rise to several atmospheres. Depending upon the design of the bulkhead structure, tank failure may occur in such "overpressure" cases. The overpressure hazard and the criteria for controlling it are being analyzed by Arthur D. Little, Inc. (ADL) as part of contract No. DOT-CG-42,357-A. Based on this study, we have formulated a procedure to evaluate the overpressure of any given cargo transfer operation, based on cargo properties, loading rate, tank characteristics, and vent system. Design and operational guidelines are suggested to avoid overpressurization. The procedure and guidelines are described in this report, along with the engineering analyses which support them.

Summary of Findings

Based on a review of ABS rules and structural analyses of decks and bulkheads of specific barges and tankers, we estimate that failure of cargo tanks occurs at pressures exceeding about 6 psig.

Typical venting systems in use today have more than adequate capacity for gas venting but inadequate capacity for liquid overfill. For example, the predicted pressure rise during gas venting does not exceed 6 psig

unless (a) the effective L/D of the vent system is about 6,000 (more than ten times the normal value) or (b) the loading rate is three times normal. The combinations of loading rate and effective L/D which lead to hazardous tank pressures are given in Table IV-2 (page 41). Cargo volatility has a relatively small effect on the hazard evaluation; a typical volatile cargo adding less than 2 psig to the normal pressure differential.

An analysis of the pressure buildup during overfill suggests that the maximum permissible ratio of loading rate (ft^3/sec) to vent cross-sectional area (ft^2) is 9 ft/sec. Many cargo transfer operations currently equal or exceed this value, having ratios of 30 ft/sec and greater in order to meet reasonable vessel turnaround times. Furthermore, tank failure is expected within a very short time (less than 30-seconds) after the tank becomes liquid full. Therefore, it appears that the liquid overfill situation must be prevented before it occurs rather than taking action after it occurs.

Arthur D Little Inc.

II. REVIEW OF NORMAL CARGO TRANSFER OPERATIONS

A. Tank Configurations

The cargo space of chemical tankers and barges is partitioned into 10 to 30 individual tanks, both for structural reasons and in order to segregate different cargoes. Ranging from 500 to 70,000 DWT in total displacement and with a typical size in the range 35,000 to 40,000 DWT, "drugstore" tankers are an order of magnitude lower in capacity than crude oil carriers. A typical individual tankship tank volume is about 12,000 bbl or 60,000 ft^3. About 50 chemical tankers of under 10,000 DWT are currently being built (Farrell [1974]). The tank and piping layout of a typical chemical tanker is shown in Figure II-1.
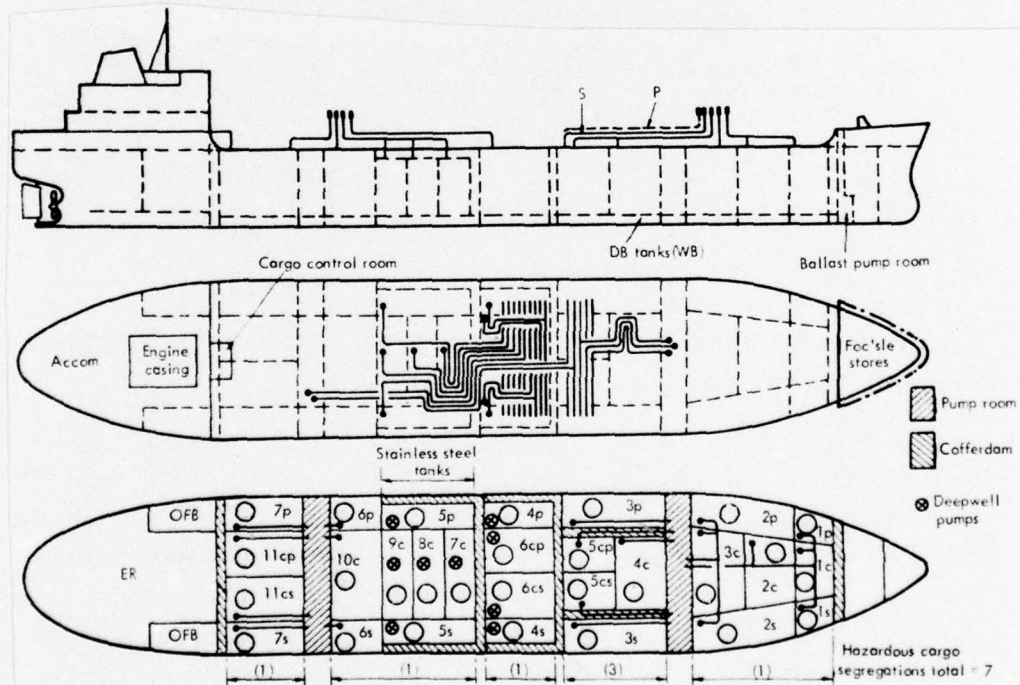

Figure II-1 – Typical Cargo Segregation Arrangement
for Chemical Tanker

(Farrell [1974])

In addition to the 200 billion ton-miles of yearly U. S. freight transport by tanker, an equal or greater amount of transport was done by about 2,500 barges used on Great Lakes and inland waterways, with a capacity ranging from 7,000 to 40,000 bbls. An individual tank on a barge would nominally be about 2,000 bbls or 11,000 ft^3. The tank layout of a typical 250 x 50 x 12 ft barge is shown in Figure II-2.

Each Tank 2,700 bbls or 15,000 Cu. Ft.
Barge Dimensions 250 x 50 x 12 Ft.
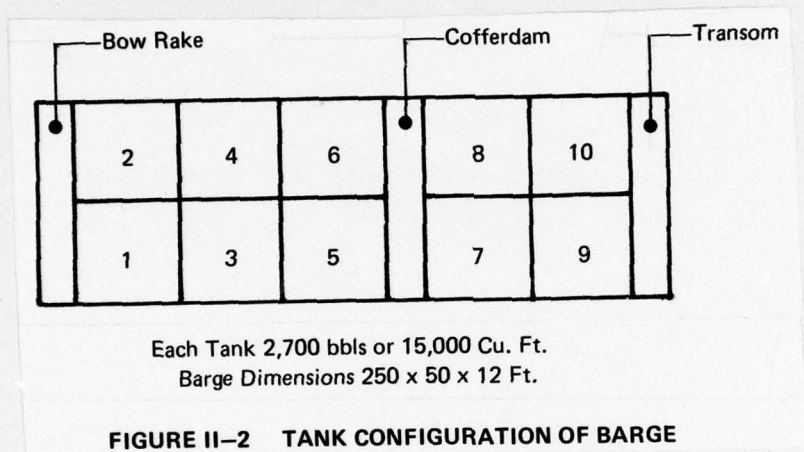
FIGURE II—2   TANK CONFIGURATION OF BARGE

B.   Cargo Transfer Procedures

Normally, the tanks, piping, and pumps are matched and sized to complete loading or offloading of the entire vessel within approximately 5 to 10 hours. The tanks are loaded by subgroups of about four tanks to each piping manifold. Based on the tank sizes noted in Section II-A, the cargo transfer rates are normally about 1,500 bbl/hr per tank for a 12,000 bbl tank on a tankship and 2,500 bbl/hr for a 20,000 bbl barge. The pumping rate for a given vessel size is shown in Figure II-3.

For most tankers and barges, the loading pumps are on-shore, but off-loading pumps are part of the vessel's equipment. In both cases, the cargo transfer operation requires adequate communication between vessel crewmen and shore pump operators. Recently, a move toward automation of dockside operations has been clear, with increased responsibility on the vessel crew. In some operations the cargo supply hose is connected sequentially to two or more cargo transfer headers.
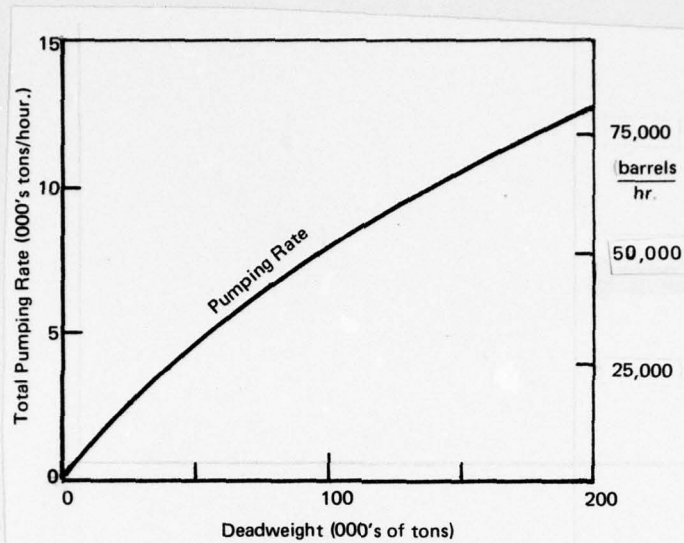
FIGURE II-3 PUMPING RATES FOR TANKERS
(Paterson and Watson [1974])

C. Key Cargo Properties

The cargoes carried in bulk can be divided into six major classes
(Farrell [1974]):

- Paraffin-based
  (Aliphatic)

ethylene	methane
vinyl chloride	acrylonitrile
formaldehyde	butadiene
propylene	naphtha
	acetaldehyde

- Aromatic-based

coal tar	toluene
naphthalene	xylene
benzene	styrene

- Alcohol-based

  | ethanol | propanol |
  | methanol | butyl alcohol |

- Ester-based

  | ethyl acetate |
  | vinyl acetate |
  | butyl acetate |

- Inorganics

  | acids |
  | soda |
  | sulphur |

- Mixtures

  | crude oil | kerosine |
  | gasoline | lubricating oils |
  | mineral spirits |

Two properties relevant to the hazards of excessive vapor displace-
ment and liquid overfill are the vapor pressure and viscosity, respectively.

5

In Table II-1 are collected the vapor pressure and liquid viscosity of
many bulk cargoes of concern.

Table II-1
Properties of Bulk Cargoes

Chemical	Vapor Pressure (Psia @ 100 F)	Liquid Viscosity (cp @ 100 F)
Acetonitrile	3	–
Allyl Chloride	11	–
Benzene	3.2	.5
t-Butyl Alcohol	1.8	1.8
i-Butyraldehyde	6	.35
Cyclohexane	3	.7
Diethylamine	7.7	.3
Diisobutylene	1.7	–
Distillate (Straight Run)	1.7	.35
Ethyl Acetate	3.1	.37
Ethyl Alcohol	2.1	–
Ethyl Benzene	0.4	.54
Ethyl Ether	18	.2
Ethylene Glycol Dimethyl Ether	2.2	–
Gasoline	Boils at 100 to 400 F	.35
Heptane	1.7	–
Hexane	5	.30
Hexene	6	.22
Isoamyl Alcohol	0.2	2.6
Isopropyl Alcohol	1.8	–
Isohexane	7	.25
Isopentane	Boils at 82.2 F	.23 @ 70 F
Isoprene	Boils at 93.4 F	.2 @ 80 F
Isopropyl Acetate	2	.41
Methly Acrylate	3	.4
Methyl Alcohol	4.5	–
Methyl Ethyl Ketone	3	–
Methyl Methacrylate	1.5	.45
Mineral Spirits	0.1	2.6
Naphtha	0.1	2.6
Oil-Penetrating	0.1	2.8
Pentane	Boils at 98.0 F	.23 @ 78 F
Pentene	Boils at 85.8 F	.20 @ 68 F
Propionaldehyde	6.7	.30
Toluene	1	.48
Vinyl Acetate	3.7	.37

D. Vent System and Constrictions

Two types of vent systems are found on cargo vessels; these are termed masthead and standpipe systems. In the masthead vent system, shown in Figure II-4, groups of tanks are manifolded to a common header which runs along the deck and up the kingpost or mast to a height which may exceed 1/3 the vessel beam. Spill valves may be installed where the smaller pipes join the header and at the base of the vertical riser to prevent overfilling to the top of the outlet. A flame arrestor or PV valve may be placed in the vertical riser. The masthead system is more prevalent for older vessels, more effective for dispersing cargo vapors, less economic for larger vessels, and is required by Regulation 46 CFR 32.55-20 (b) for Grade A liquid cargoes.

The standpipe system, illustrated in Figure II-5, consists of a vertical vent pipe above each tank designed to release excessive vapor in mixture at a height of 3 to 8 ft above deck level. The pipe is normally fitted with a PV relief valve, a flame control device, and a gooseneck to protect against weather. The standpipe system is common on newer tankers, larger tankers, and almost all barges.

Both vent systems present a finite constriction to the gas efflux when the P-V valve is open. The vent pipe diameters, which range from 2-1/2" to 12", are sized according to the anticipated displacement rates, which in turn are limited by the size of the cargo filling lines due to the resistance of liquid inflow. The resistance to gas outflow is several orders of magnitude less than the liquid pressure drop for a given vent system. Certain vent piping systems appear to have been sized large enough to accomodate a liquid cargo overfill; these systems are "overdesigned" for gas venting. However, as we shall point out below, for most vent systems the capacity of the P-V valves and other vent fittings generally are marginal for liquid flow, giving rise to pressure drops of several atmospheres during an overfill. That is, many vent systems appear to have excess capacity for gas venting and inadequate capacity for cargo overfill.

The *effective* length-to-diameter ratio, L/D, is a convenient index of the constriction presented by a vent system to either liquid or vapor flow. In pressure drop calculations, the L/D is multiplied by the friction factor f; the latter accounting for variations in flow rate and wall roughness. We have tabulated in Table II-2 the appropriate L/D for various pipe fittings
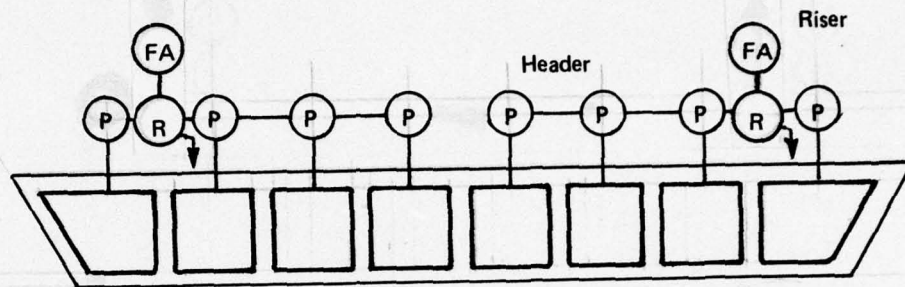
FIGURE II–4   SCHEMATIC OF MASTHEAD SYSTEM

(P) Pressure-Vacuum Valve (Sometimes Ball Check Valves Are Used On The Standpipe System)

(R) Relief or Spill Valve

(F) Flame Screen

(FA) Flame Arrestor
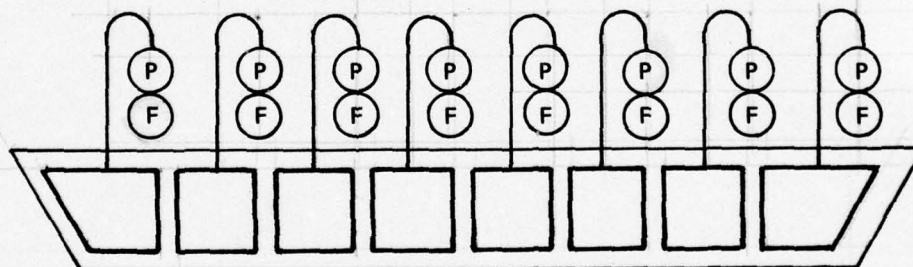
FIGURE II–5   SCHEMATIC OF STANDPIPE SYSTEM

Table II-2

Representative Equivalent Length in Pipe Diameters (L/D)
of Various Valves and Fittings

Standard Valves	L/D
Globe valves (fully open)	340
Gate valves (fully open)	13
Gate valves (1/2 open)	160
Swing check valves (fully open)	135
Check valves (fully open)	150
Butterfly valves (fully open)	20

Standard Fittings	
90 degree standard elbow	25
45 degree standard elbow	16
180 degree "U" or gooseneck	40
Standard tee	
Flow through run	20
Flow through branch	60

Vent System Components	
Flame arrestor (typical)	200 ± 100
P-V relief valve (typical)	100 ± 50

Sources: Data on standard fittings taken from Crane Company, Technical Paper 410.

Data on USCG-approved valves and flame arrestors taken from GPE, Protectoseal, and Varec catalogues.

and valves. For a masthead system, the effective L/D may reach several hun-
dred. This is indicated in Figure II-6, which is based on the vent system
of a typical 70,000 DWT tanker.

Note: This figure is for illustrative purposes only and is not intended to depict an actual arrangement.

L/D = 40 for Gooseneck

2 psi Overfill Relief

Flame Arrestor
L/D = 200

48'

L/D = 60 for Tee

12" Dia Header

100'

L/D = 25 for elbow

Ullage Opening

Fill

10'6"

6" Dia

17" Dia

P-V Valve (open)
L/D ≈ 100

L/D = 25 for Elbow

Tank

Total Effective Length to Diameter Ratio:

L/D = 171 + 473 = 644

Item (itemized from tank outlet)	Effective L/D of Branch Line	Effective L/D of Header
Elbow	25	—
Run 10.5 ft	21	—
Elbow	25	—
P-V Value	100	—
Subtotal	171	
Branch Tee	—	60
Run 100 ft.	—	100
Elbow	—	25
Flame Arrestor	—	200
Riser	—	48
Gooseneck	—	40
Subtotal		473

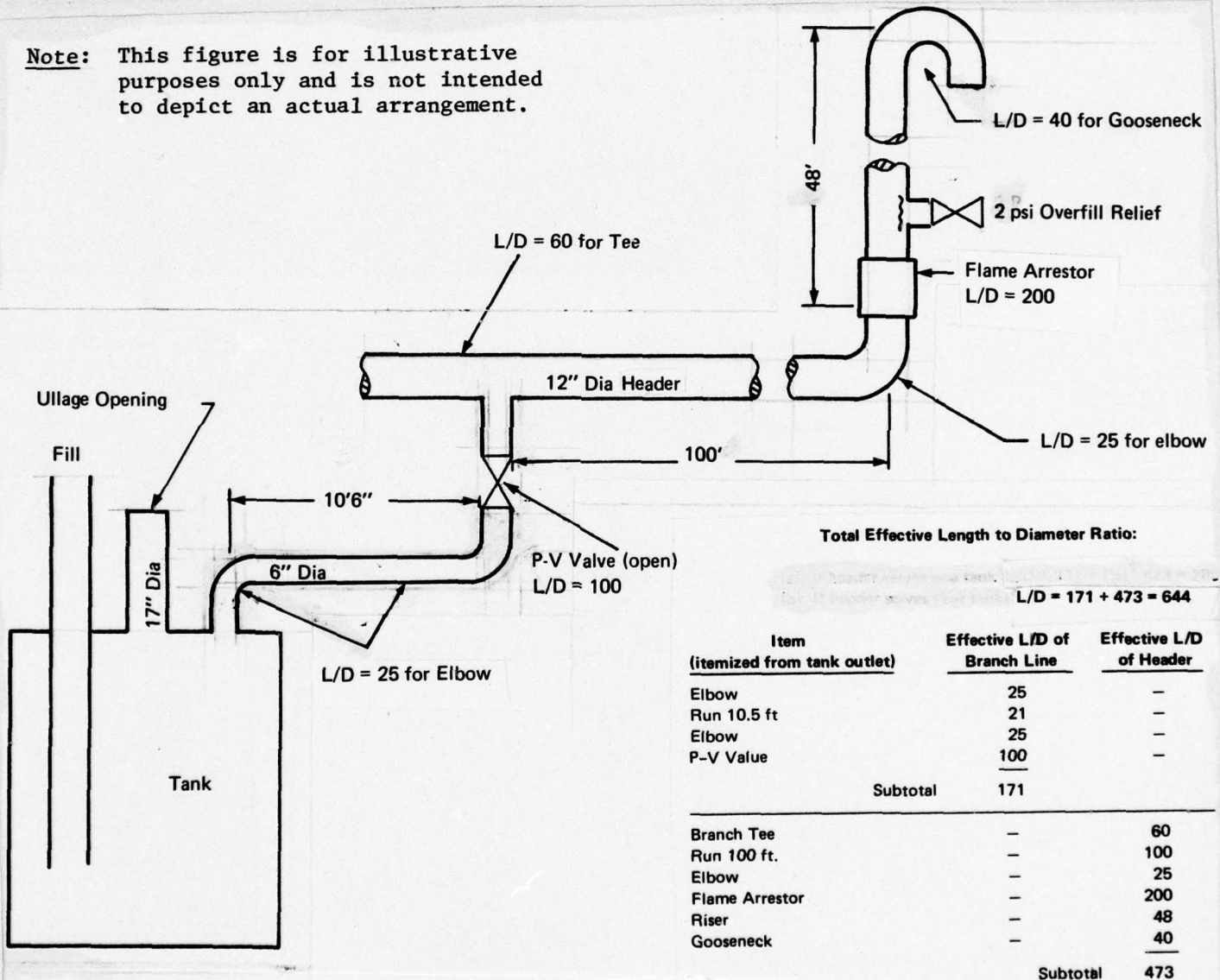FIGURE II-6   TYPICAL MANIFOLDED VENT SYSTEM

E. Normal and Extreme Cargo Transfer Situations

In the above sections we have described the tank configuration, the cargo transfer procedures, the cargoes, and the vent systems. Under normal situations ther. is no overfill, and the vent releases vapor/air mixture at 100 to 130% . he volumetric fill rate, with a tank pressure rise in the range of 0 to 3 psi above ambient. The normal efflux velocity under these conditions is in the range of 10 to 40 ft/sec (Paterson [1974]).

Overpressure can occur either by (a) inadvertently overfilling the tank and attempting to force liquid cargo through the vent system or (b) using fill rates which are excessive for the finite constriction of a given vent system. The parameter values of these two extreme cargo transfer situations are contrasted to the normal values below in Table II-3.

Overfill is a widely recognized problem and was cited as a contributing factor in the gasoline fire and explosions of tank barge "Ocean 80" in Carteret, New Jersey, in 1972 (USCG/NTSB-MAR-75-3). In this case, however, overfill did not cause overpressurization. Apparently this particular barge was designed to accomodate overfill. The tolerance for error on the part of the tankermen or dockside pump operators is very narrow indeed, without improved gauging devices, high-level alarms, spill valves, or overfill tanks.

12

Table II-3

Parameter Values for Normal and Extreme Transfer of Cargo

Parameter	Normal Range	Excessive Range	Notes
Tank fill time (tank volume/volumetric fill rate)	5 - 10 hr	1 - 5 hr	a
Inviscid vent pipe velocity (volumetric fill rate/vent pipe area)	20 - 40 ft/sec	40 - 200 ft/sec	b
Effective L/D	150 - 500	500 - 5,000	c
Friction factor 4f L/D	3 - 10	10 - 100	d
Cargo viscosity	1 - 100 cp	~ 100 cp	e
Cargo vapor pressure	0.1 - 10 psia	-	

Notes: (a) For example, 12,000 ft^3 barge tank filled at 1,200 - 2,400 ft^3/hr (150 - 300 gpm) or 60,000 ft^3 tank filled at 6,000 - 12,000 ft^3/hr (750 - 1,500 gpm). Excessive fill rates up to a factor of five above normal might be due to (a) wrong pump selection or (b) valves set for single tank loading rather than manifold of four tanks loaded at once.

(b) For example, 8,000 ft^3/hr displacement rate plus 1,000 ft^3/hr evaporation rate into 5 in. ID vent pipe gives 18 ft/sec efflux velocity (with P-V valve fully open).

(c) See Figure II-6. The standpipe vent of 6 in. ID has an L/D of about 170. The masthead vent has an L/D of about 470 for gas venting.

(d) Fanning friction coefficient f ≈ .005 according to Bird, Stewart, and Lightfoot, Transport Phenomenon, Wiley, p. 182ff.

(e) Viscosity is shown at an assumed 80°F loading temperature rather than at 100°F.

13

Arthur D Little Inc

III. ESTIMATION OF TANK FAILURE PRESSURE

A. General Discussion and Results

Estimates were made of the minimum internal pressure loadings required to initiate failure of cargo tanks of three representative vessel designs: an offshore barge, an inland barge, and a large tankship. The approach used to develop these estimates consisted of elastic structural analyses of the deck and sides of the cargo tanks, and, where appropriate, the bottom and bulkhead structures. The analysis was based on the work of Clarkson (1965) on plated flat grillages, augmented by the orthotropic plate methods of Schade (1940) and Lekhnitskii (1968).

In all cases, the structural resistance of the plating between the longitudinal and transverse framing members was found to be considerably higher than the resistance of the framing members them-selves, so that the minimum failure pressure loadings were defined by the stress levels developed in the framing members.

The intent of this analysis was to determine, using simplified structural models of the cargo tanks, a range of pressure levels at which typical cargo tank configurations would be expected to fail. These pressure levels have been utilized to establish the overpressure hazards for the range of cargo venting and loading rates of interest to this overall study program. It was not the intent of this analysis to conduct a detailed study of the response of cargo tank structures to the various static and dynamic loadings, residual stresses, or thermal effects normally considered in detailed design analysis. Such additional stresses in the cargo tank structure have been accounted for in an approximate fashion by assuming as the failure criterion the attainment of yield stress levels (rather than ultimate stress) in the tank structure due to the internal pressure loading alone. The stresses developed due to the other loadings were, therefore, assumed to be sufficient, when added to the yield stress, to produce ultimate stress levels at one or more locations in the highly redundant structure.

The accuracy resulting from this assumption and from the elastic structural analysis is expected to be about ± 30%.

For the purposes of this study, the Coast Guard has provided structural data on the cargo tanks of the three representative vessels.

On the basis of our analyses on the three vessels, it has been calculated that an average internal pressure level in the cargo tanks of about six psig will be sufficient to initiate failure of the cargo tank structure. This level represents an average of about eight psig for the tankship, six psig for the offshore barge, and about four psig for the inland barge. A summary of the results is given in Table III-1. For each of the three vessels analyzed, the weakest portion of the tank structure (the probable location of initial failure) was determined to be at the ends of the transverse frames at the tank boundary defined by the deck-sidewall intersection.

B. Structural Analysis Methods

Many ship structures are in the form of plated grillages, in which stiffening beams in either one or two directions (generally orthogonal) are attached to the plating to provide resistance to lateral loadings. Such structures are commonly used in the decks, sides, bottoms, and bulkheads of ships; and also find applications in civil engineering structures and in aircraft structures. Grillages of these types are highly redundant structures, so that they cannot be analyzed by static equilibrium methods alone; the additional conditions relating to the compatibility of the deflections of the structural components must be imposed.

For most grillage structures used in marine cargo tanks, there are generally several stiffening beams (longitudinal and/or transverse members) so that the overall structure has a large number of redundancies. Direct solution by hand of the stresses and deflections, using indeterminate analysis methods, is extremely cumbersome for grillages of any significant complexity, with the

15

Arthur D Little Inc

TABLE III-1

SUMMARY OF CARGO TANK FAILURE PRESSURES

Cargo Vessel	Structure	Failure Pressure (PSI)	Remarks
Offshore Barge	Deck	6*	Transverse Beam
	Deck Plate	13	
	Bottom	10*	Transverse Beam
	Bottom Plate	13	
	Side	10*	Transverse Beam
	Side Plate	13	
	Trans. Bulkhead	14	Horizontal Stiffness
	Bulkhead Plate	15	
	Long. Bulkhead	10*	Transverse Beam
	Bulkhead Plate	15	
Inland Barge	Deck	3*	Transverse Beam
	Deck Plate	11	
	Bottom	4*	Transverse Beam
	Bottom Plate	16	
	Side	3.5	Transverse Beam
	Side Plate	16	
	Trans. Bulkhead	7	Vertical Stiffener
	Bulkhead Plate	11	
	Long. Bulkhead	12	Vertical Stiffener
	Bulkhead Plate	11	
Tankship	Deck	12	Transverse Beam
	Deck Plate	70	
	Side	8	Transverse Beam
	Plate	24	

* Based on average of upper and lower limit structural models of tank
   structure to account for interior trusswork. See text.

16

Arthur D Little Inc

development of computer methods, however, such analyses have been carried out in parametric form for a range of structural configurations. The work of Clarkson (1965) has included study of flat grillages under uniform lateral pressure (which is the loading of principal concern for the present program) for several cases of odd numbers of stiffening beams, up to orthogonal sets of 15 x 9 beams. The boundary conditions studied have included opposite edges either fixed or simply supported. The plating, which in most ship grillages is welded to the stiffening members, is assumed by Clarkson to behave as an effective flange to the transverse and longitudinal members, so that the structural model is essentially reduced to a gridwork of intersecting beams.

One of the difficulties in applying Clarkson's work is the relatively limited range of stiffness ratios studied. Many ship structures of current design, including in particular bulkheads in oil tankers, and decks and sides of longitudinally-framed tankers, consist of relatively heavy and wide-spaced transverse members and relatively light longitudinal members. In addition, some bulkhead structures are typically stiffened in one direction only.

In some of the particular grillage structures analyzed in this study, it was found that the Clarkson data could be extrapolated to provide reasonable results; in other cases, the extent of extrapolation needed was too large to provide meaningful answers. An alternative method for analysis of grillages is to model the stiffened structure as an orthotropic plate, in which the stiffening members are transformed into a continuous structure having an equivalent stiffness per unit width in each of the two orthogonal directions. Once this is done, the solutions of orthotropic plate analysis can be applied, or for cases in which the stiffeners and their spacing are the same in both directions, the solution of the flat plate analyses can be used.

One difficulty with the orthotropic plate approach is that only a limited number of sets of boundary conditions have been formally

Arthur D Little Inc

solved. The solution for the case with all boundaries fixed, for example, has not been developed. Estimates for the fixed-boundary case can be made, however, from some of the other configurations which have been studied, both theoretically and by approximate methods. An orthotropic plate procedure was programmed and used in the present study to develop estimates for those grillage structures for which Clarkson's data sheets could not be used. It was also used to check the results for those cases in which the Clarkson data sheets were applicable either directly or by relatively minor extrapolations.

C. Offshore Barge Structural Analysis

1. Dimensions

The offshore barge chosen for analysis was a Todd 605 design of overall dimension 376 feet by 78 feet by 31-3/4 feet. The largest cargo tank is 56 feet long, 37 feet wide, and 31-3/4 feet deep. The deck, sidewall, bottom, and longitudinal bulkhead structures of the tanks are orthogonally-stiffened with relatively small and close-spaced longitudinal members, and with relatively heavy transverse members spaced eight feet on center. These transverse members, which are notched over the longitudinals and welded directly to the plating, are part of a transverse truss structure consisting of (1) two stanchions spaced at thirteen foot intervals and (2) diagonal members from the top and bottom of each stanchion to the center height of the sidewall and the longitudinal bulkhead. Such transverse truss structures are typical of many barge designs.

The transverse bulkhead structure is also stiffened in both directions with closely-spaced horizontal members and heavy widely-spaced vertical members.

2. Methods of Analysis and Results

Each of the major structures of the cargo tank was analyzed in two ways: with the grillage methods of Clarkson and with an ortho-tropic plate method. The presence of the truss systems within the

18

tank complicates the modeling of the deck, bottom, sidewall, and longitudinal bulkhead structures in that the truss contributes significantly to the resistance of these structures to lateral pressure loadings. An accurate determination of the effect of the truss structure in this regard would require a modeling of the three-dimensional configuration of the grillages and trusses in terms of one of several available finite-element computer codes, such as NASTRAN or STARDYNE. Such a procedure is clearly well beyond the scope of this program. An alternative procedure which was followed here was to attempt to bracket the actual structural configuration by analyzing simplified configurations. These simplified models included one in which the out-of-plane truss members were ignored (this model would tend to predict much lower critical pressures than the actual structure); another in which the transverse section of the plane of the truss was assumed to be infinitely stiff, so that the structure analyzed, by an orthotropic formulation, consisted of a plate reinforced in one direction only, and having a longitudinal dimension equal to the truss spacing (this model would result in higher critical pressures than the actual structure). Still another model analyzed was a grillage structure whose length was equal to the full tank length, but whose width extended to the stanchion only. This structural approximation, which was based on the assumption that the truss stanchions defined a fixed longitudinal line, would also result in prediction of higher critical pressures than the actual structure could resist.

As an example, the entire deck structure of the barge, when analyzed without the contributions of the interior truss members, is calculated to develop yield stress levels in both the longitudinal and transverse members at a uniform lateral pressure of about two psi. When analyzed with the transverse sections fixed, yield stress levels would develop at a uniform lateral pressure of about nine psi. Analysis of the reduced deck structure, assuming a fixed stanchion line, results in a lateral pressure level of about ten psi in the

19

longitudinal members and about 18 psi in the transverse members.
A realistic value is obviously above two and below nine, and has
been assumed to be six psi.

Similar approaches used for the bottom, sidewall, and longitudinal
bulkhead structures have resulted in probable values for the critical
lateral pressure equal to 10 psi or more. Calculations for the trans-
verse bulkhead led to an estimate of 14 psi for the critical
pressure.

For completeness, the lateral pressure levels necessary to develop
yield stress in the individual areas of plating, i.e., the rectangular
plate segments defined by the grillage members, were also calculated.
Assuming fixed boundary conditions, the critical pressures were in
excess of 12 psi.

Thus, the critical internal pressure for the cargo tanks of this
offshore barge design was taken to be six psi, corresponding to the
development of yield stress in the barge tankage structures, reached
initially in the transverse members at the deck sidewall intersection.

D.   Inland Barge Structural Analysis

1.   Dimensions

The inland barge design studied was a single-skin oil barge,
NBC Hull 1654. This vessel has overall dimensions of 132 feet by 50
feet by 10-1/4 feet, with a typical cargo tank having dimensions of
51 feet by 25 feet by 10-1/4 feet. The tank structures are longi-
tudinally stiffened, with transverse frames, also in the form of
trusses, spaced at approximately 7-1/2 foot intervals. The transverse
members are welded to the flanges of the longitudinals, and thus are
not attached directly to the plating. The truss system includes, in
addition to the top, bottom, and sidewall members, three stanchions
spaced at 6-1/4 feet intervals. Diagonal members extend from the
bottom of the sides and from the bottom of the middle stanchion to the
top of the adjacent stanchions, thus forming an inverted W across the

20

Arthur D Little Inc

tank section. Both the longitudinal and transverse bulkhead structures
are stiffened in the vertical direction only.

2. Methods of Analysis and Results

Both the grillage methods of Clarkson and the orthotropic plate
approximations were used to analyze the various structural elements
of the inland barge. As in the case of the offshore barge, the
analyses of the deck, bottom and sidewall structures were based on
simplified models; the first model neglecting the resistance offered
by the out-of-plane truss members, another model based on the assump-
tion that the transverse frame was infinitely stiff, and a third model,
where appropriate, using the reduced width as defined by the stanchion
spacing. These simplified structural models can reasonably be
considered to bracket the resistance of the actual grillage and truss
structures.

For the deck structure, the analysis of the entire deck without
contributions from the interior truss members led to values of maximum
lateral pressure of about one-half of a psi for initiation of yielding
in the transverse members, and about one psi for the longitudinal
members. Assuming that the transverse members (top elements of
interior truss structure) were fixed, yield stress levels were reached
in the longitudinal members at about 13 psi. Finally, the model based
upon the width of deck equal to the spacing of the stanchions led to
critical lateral pressure levels of about eight psi for the transverse
members and 11 psi for the longitudinals.

A reasonable mean value for the critical lateral pressure for the
deck structure would be three psi.

Similar sets of calculations for the sidewall and bottom structures
indicated that the critical pressure range for the sidewall was 3-1/2
psi for yield stress in the transverse members, and for the bottom, a
mean value of about four psi appears reasonable.

The bulkhead structures of this barge design, each of which is stiffened in the vertical direction only, were analyzed as orthotropic plates, and led to critical lateral pressures of greater than seven psi. The plating itself was determined to require in the worst case a minimum of 11 psi to reach yield conditions.

The rather surprisingly low values obtained for the deck, side, and bottom structures of this barge suggested that the scantlings be evaluated for adequacy and adherance to the Rules of the American Bureau of Shipping (1967, 1971). The evaluation indicated that the deck and bottom transverses were adequately sized, but that the side transverse was undersized. This condition was brought to the attention of technical staff personnel at MMT New Orleans, from whom the scantlings had been obtained, and that office concurred in this evaluation.

In view of this, it would seem reasonable to assume that the typical inland barge may be somewhat more resistant to internal pressure loadings than indicated from the analyses carried out for this particular barge design. Accordingly, it is suggested that a value of the critical internal pressure level for use in this study equal to about four psi would be appropriate.

E. Large Tankship Structural Analysis

1. Dimensions

The tankship chosen for analysis was a large vessel of overall dimensions 1075 feet by 143-1/2 feet by 91 feet deep, with a draft of 70 feet. The inboard deep tank analyzed in detail was 198-1/2 feet long, 32 feet, 11 inches wide, and of full depth. The tank was free-standing, without internal cross members or trusses, and was longitudinally framed with heavy, widely-spaced web frames.

2. Methods of Analysis and Results

The deck and sidewalls (which in the case of the inboard tank also serve as the longitudinal bulkhead structures) were analyzed using extrapolated values from the Clarkson grillage charts, and were

Arthur D Little Inc

then verified using the orthotropic plate formulation. Extrapolations
to the Clarkson charts were necessary because of the relatively large
web frame structures used in the tanks, which effectively resulted in
a very high ratio of the transverse to longitudinal stiffness of both
the deck and sidewall grillages.

The results for the tank ship indicated that yield stress levels
would be developed at the upper end of the transverse web frame of
the sidewall under an internal lateral pressure of about eight psi,
in the transverse member of the deck structure at about 12 psi, and
in the longitudinals of the deck and sidewall structures of 26 and 13
psi, respectively. Yield stress levels in the plating itself requires,
as in the cases for the barge tankage, higher lateral pressures than
those associated with the development of yield stress in the grillage
members. Assuming fixed boundaries, lateral pressure levels of 24
and 70 psi would be needed to reach yield stress in the sidewall and
deck plates, respectively. On the basis of these results, it would
appear that a reasonable assumption for the value of the critical
internal pressure for large cargo tank structures would be eight psi.

10 Lines
to End of
Typing Area

IV. TANK PRESSURE RISE DURING LOADING

A. Factors which Contribute to Pressure Rise

Having an estimate of the tank failure pressure, we seek to deter-
mine the maximum pressure reached during cargo transfer operations,
and when it is reached. As illustrated in Figure IV-1, this will make
it possible to recognize hazardous cargo transfer situations. The ob-
jective of the analysis presented is to predict the pressure history
inside a tank when it is being filled with a liquid. The pressure rise
results from the finite pressure drop of the vents provided to discharge
the vapor/air displaced by the liquid which is filling up the tank.
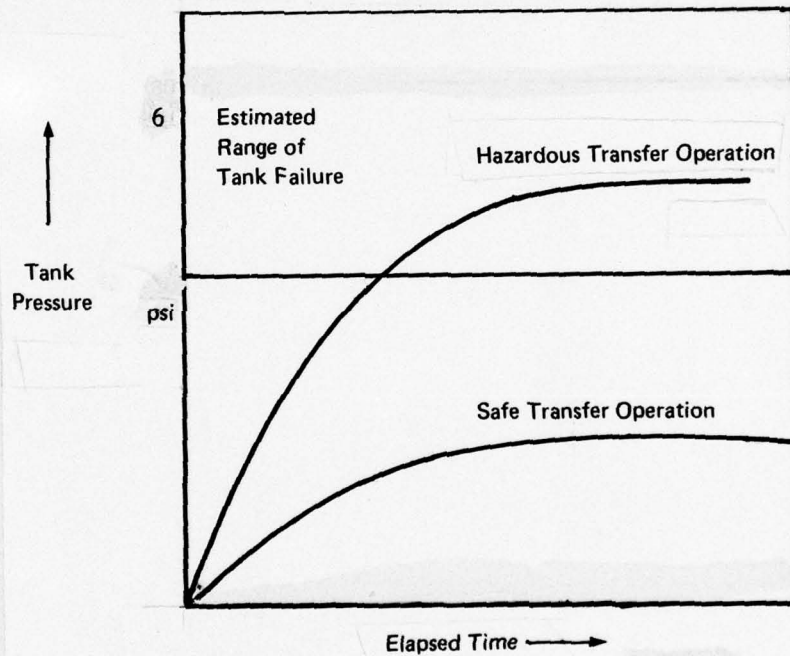
FIGURE IV-1 SCHEMATIC OF PRESSURE HISTORY

In general, (as will be shown) the venting capacity is adequate to
discharge the gas mixture, without creating back pressures in excess
of a few psig. However, if the relief valve is stuck for some reason
or if the vent area is reduced to blockage, or if the loading rate is
excessive, or if the cargo evaporates vigorously during loading, there
results a compression of the vapor/air mixture in the tank resulting in
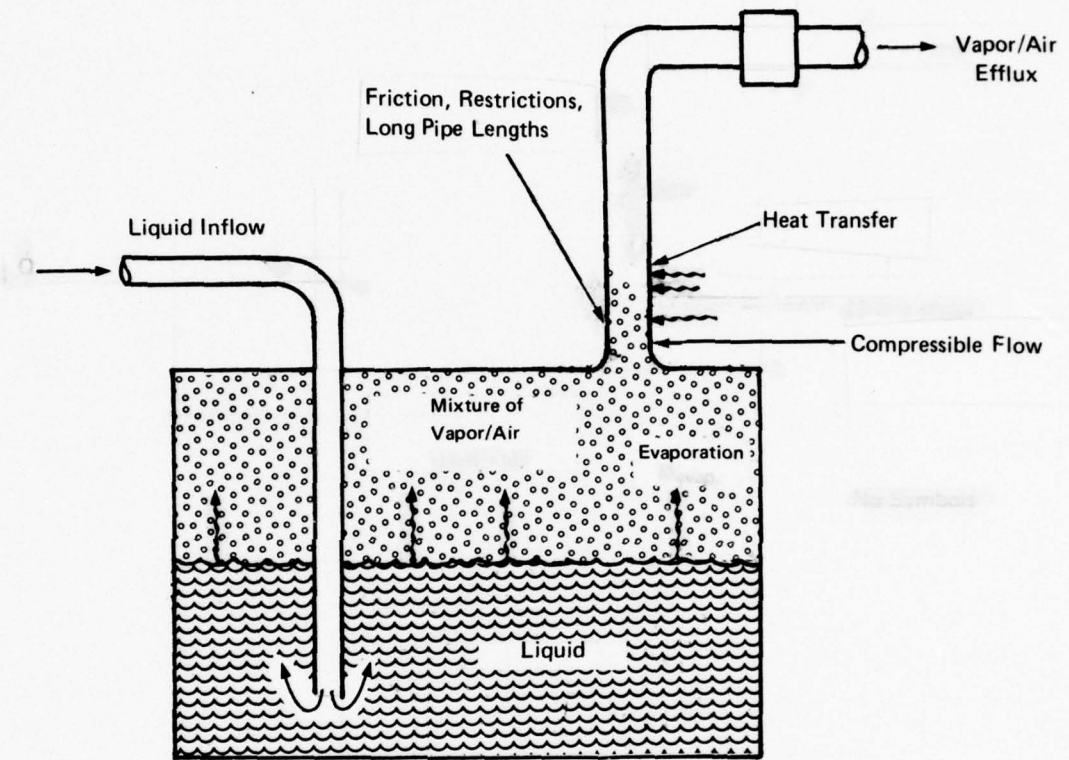hazardous tank pressures. Some of these factors are shown in Figure IV-2.

FIGURE IV-2   SCHEMATIC DIAGRAM SHOWING FACTORS IMPORTANT TO PRESSURE RISE

B. Cargo Evaporation Rate

The phenomena of evaporation and mixing of vapor with air during loading affects the pressure rise. The description of evaporation is in general exceedingly complicated and demands that simplifying assumptions be made. Consider the bottom loading (of liquid) configuration shown in Figure IV-3. Just before the liquid is let in, the tank volume is full of air. As the liquid comes in, it seeks to establish the equilibrium vapor pressure next to the liquid surface. Vapor is generated. If the vapor is heavier than air, it is very likely that there will be gas-air stratification. There may be an intermediate region where there will be a mixture of air and vapor with the concentration varying continuously. On the other hand, if the vapor generated is lighter than air, mixing caused by buoyancy force may occur. Thus, the key to the analysis is how the mixing process is handled. Molecular mixing** is negligible compared to turbulent mixing as a mechanism for clearing off the liquid surface of vapor. The loading pipe outlet presumably creates enough local turbulence to justify this assumption.

If molecular mixing were controlling, there would be negligible pressure rise and evaporation rate, because the tank dimension greatly exceeds the distance over which molecular diffusion can penetrate during the fill time.

Turbulent mixing is represented by a one-dimenionsal Fick's Law expression for vertical diffusion. The coefficient for eddy diffusion is set at 10^4 the molecular value: $(\epsilon = 2 \text{ ft}^2/\text{sec})$.[*] As shown in a standard text on mass transfer (i.e., Bird, Stewart, and Lightfoot, p. 594 ff, (1960)), one can derive the following expression for the mass of vapor added as a function of time:

$$M_{vap} = \frac{\rho_{vap} \, p_{vap}}{p} \, S \sqrt{\frac{4 \, \epsilon \, t}{\pi}} \tag{1}$$

where S is the surface area of liquid and p_{vap} the equilibrium partial pressure of vapor (taken at the liquid cargo temperature). The rate of evaporation is obtained by differentiation of Equation (1) with respect to time:

---

[*] This is quite conservative (more mixing than actually expected) because the eddy transport properties are commonly taken at 100 to 1000 times the molecular values.

**Molecular mixing occurs in a stagnant gas and thus differs from turbulent mixing.

26

Liquid Cargo

Efflux

Vent System

Zone of Pure Air

Vapor-Air
Mixing Zone

Vapor is of
Different
Molecular Weight
Than Air

Zone of Saturated Vapor Pressure

Heat of Evaporation Reduces Liquid Surface
Temperature

Splashing Increases Exposed Liquid
Surface Area

Liquid Surface Area Increases as
Liquid Spreads Across Tank
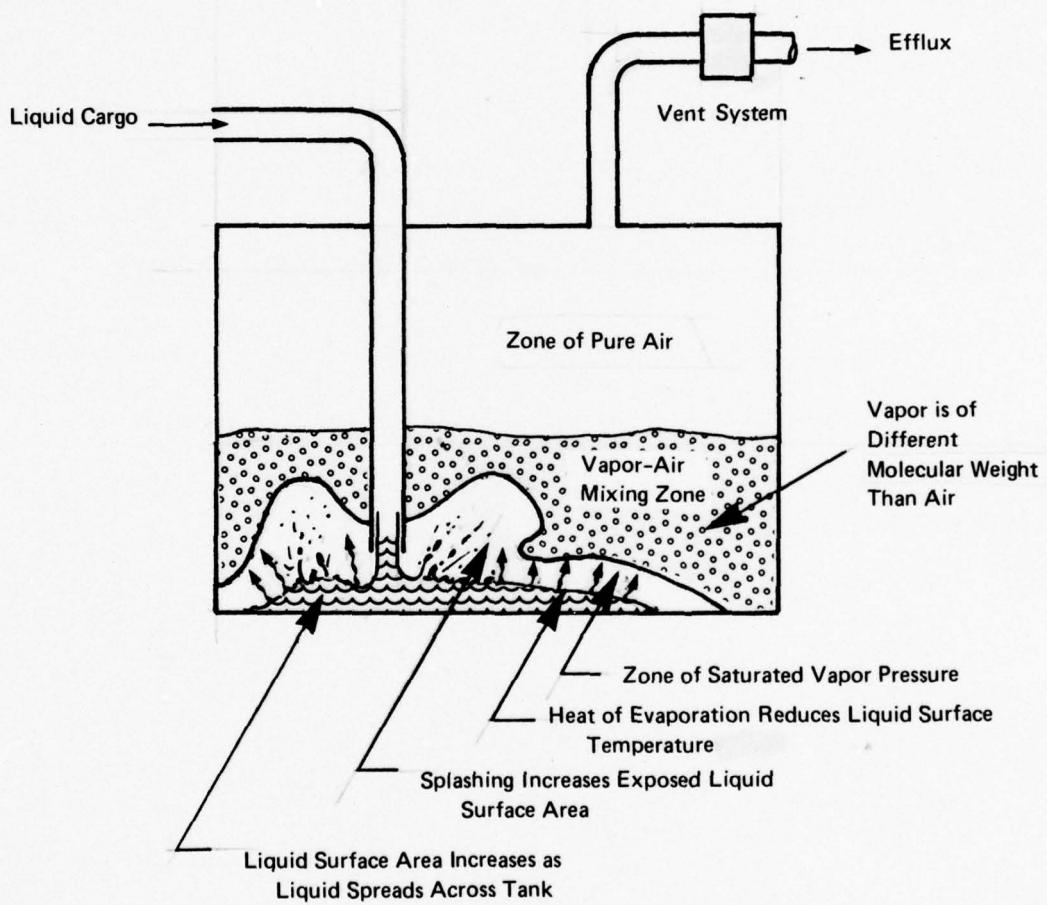
FIGURE IV-3   SOME PHYSICAL PROCESSES WHICH
AFFECT THE EVAPORATION RATE

$$\dot{M}_{vap} = \frac{\rho_{vap} \, p_{vap} \, S}{2p} \sqrt{\frac{4\varepsilon}{\pi t}} \left(1 - \frac{2t \, dp/dt}{p}\right) \tag{2}$$

The analysis was carried out omitting the correction term $2t(dp/dt)/p$, which ranges between .002 and .02 for the parameter values of interest. Furthermore, the pressure p in the denominator of Equation (2) was taken to be a constant equal to the tank pressure when loading is complete, $p(t_{fill})$. This is consistent with omitting the correction term ($dp/dt = 0$ implies $p =$ constant). Essentially, the net effect of these two changes is to omit the effect on evaporation of the increase in ullage pressure during the cargo loading process.

Since Equation (1) suggests $\dot{M}_{vap} \sim p^{-1}$, taking $p = p(t_{fill})$ will underestimate the mass of vapor added since $p(t_{fill}) \geqq \bar{p}(t)$. However, this simplification is justifiable in view of the other coarse assumptions imposed on the evaporation analysis (see below). The actual variation of p which we have omitted in Equation (1) is much less than the uncertainty in the diffusion coefficient ε. The expression actually adopted in the analysis is based on evaporation into a tall uncovered tank:

$$\dot{M}_{vap} = \frac{\rho_{vap} \, p_{vap} \, S}{2p(t_{fill})} \sqrt{\frac{4\varepsilon}{\pi t}} \tag{3}$$

In the calculations of tank pressure, it will be convenient to use the ratio K of volumetric evaporation rate ($\dot{M}_{vap}/\rho_{vap}$) to the volumetric loading rate $\dot{Q}$. The ratio K must be referenced to a particular time since $\dot{M}_{vap}$ decreases as $t^{-1/2}$. For convenience, we take the reference time as the fill time, t_{fill}:

$$K \equiv \left(\frac{\text{EVAP. RATE}}{\text{LOADING RATE}}\right)_{t_{fill}} = \frac{\left[p_{vap}/p(t_{fill})\right] S \sqrt{4\,\varepsilon/\pi}}{2 \, \dot{Q} \, t_{fill}^{1/2}} \tag{4}$$

A sample value of K can be obtained as follows: substituting $\varepsilon = 2 \text{ ft}^2/\text{sec}$, $\dot{Q} = 5 \text{ ft}^3/\text{sec}$, $t_{fill} = 4 \text{ hr}$, $S = 500 \text{ ft}^2$, $p_{vap} = 5 \text{ psi}$, and $p(t_{fill}) = 6 \text{ psi}$, we obtain

$K = .55$

Values of K ranging from 0.1 to 0.7 were considered in the analysis in order to explore larger values of the liquid surface area S and the diffusion coefficient ε.

Substituting Equation (4) into Equation (3), and assuming $\rho_a = \rho_{vap}$, we obtain the working expression for evaporation rate:

$$\dot{M}_{vap} = K\, \rho_a\, \dot{Q}\, (t_{fill}/t)^{1/2} \tag{5}$$

Additional complications arise (a) if the vapor is hotter or colder than initial air, (b) if there is a cooling effect of evaporation due to latent heat, or (c) if the actual exposed liquid surface area varies due to a jet from the fill pipe or spreading across the tank floor. Here we neglect all of these complications by assuming that:

- Cargo loading temperature is close to ambient;

- Liquid surface stays at the cargo loading temperature (which is known); and

- Constant exposed liquid surface area equal to tank floor area.

C. Mathematical Model of the Venting Process

Mathematical models have been developed which describe the pressure as a function of time for given cargo transfer conditions. The model presented below includes the effects of gas compressibility, vent system friction and restrictions, cargo evaporation, loading rate, and heat transfer from the ambient to the gas in the vent system.

1. Assumptions

(a) Gas properties: The entire analysis is performed assuming that the vapor/air mixture being vented has the molecular weight, specific heat, and viscosity of pure air. In the case of high vapor pressure liquids, there will be substantial evaporation into the tank, and if the vapor differs substantially from air, this assumption will not be strictly valid.

(b) Liquid loading rate is constant.

(c) Tank volume is fixed - i.e., we neglect tank expansion.

(d) The friction coefficient for the venting system is a constant (that is, the flow through the vent is in the high Reynolds Number - turbulent flow regime).

(e) Vent flow is isothermal: Heat exchange occurs between the ambient and the gas flowing in the vent system to the extent that the

gas temperature variations are negligible. An alternate model based on adiabatic flow is presented in Appendix A.

(f) Evaporation rate is limited by turbulent vertical mixing in the tank, so that the mass addition rate is proportional to the inverse square root of elapsed time.

(g) Initial conditions within the tank are the same as the ambient conditions.

(h) The mass of vapor is assumed small compared to the liquid cargo mass, even at earliest stages of loading.

2. Analysis

First a mass balance equation is written for the vapor mass in the tank as a function of the outflow rate and the evaporation rate. Then from the vent characteristics, the outflow rate is expressed as a function of the tank pressure. The evaporation rate, Equation (5), is also used in the mass balance. The resulting equation for tank pressure is complicated and must be solved simultaneously.

Taking a mass balance on the vapor/air mixture, we obtain:

$$\frac{dM}{dt} = -\dot{M}_v + \dot{M}_{vap} \tag{6}$$

| Rate of change of air/vapor mass in the tank | Mass rate of venting | Mass added from evaporation |

Equation (6) is the fundamental equation determining the pressure rise. Each of the three terms will be expressed in terms of tank pressure. The left-hand side is developed as follows. For a compressible gas, the mass of the air-gas mixture is

$$M = \rho V = \rho_a V_T \left(\frac{\rho V}{\rho_a V_T} \right) \tag{7}$$

For constant loading rate, $V/V_T = 1 - t/t_{fill}$, and for an isothermal gas, $\rho/\rho_a = p/p_a$; therefore, Equation (7) becomes

$$M = \rho_a V_T (p/p_a)(1 - t/t_{fill}) \tag{8}$$

Next, the venting rate $\dot{M}_v$ is to be related to the pressure rise. The relationship between pressures on the upstream and downstream side of the vent and the mass flow rate can be derived for isothermal flow from Shapiro,[13] eq. (6.42) on page 182:

$$p^2 - p_a^2 = \left(\frac{\dot{M}_v}{A}\right)^2 RT \left[2 \ln (\rho/\rho_a) + 4f \frac{L}{D}\right] \tag{9}$$

where R is the gas constant.* Values of the Fanning friction factor for fully developed turbulent flow under typical venting conditions range from 0.004 to 0.006 with a typical value of about 0.005.

Substituting $\rho/\rho_a = p/p_a$ and solving for $\dot{M}_v$, we obtain

$$\dot{M}_v = \frac{(P^2 - P_a^2)^{1/2} A}{(2RT)^{1/2}[\ln(p/p_a) + 2f \, L/D]^{1/2}} \tag{10}$$

In order to complete the formulation, we recall from Section IV-A that

$$\dot{M}_{vap} = K \dot{M}_c (t_{fill}/t)^{1/2} \tag{5}$$

where K is defined on page 28.

Substituting Equations (5), (8(, and (10) into Equation (6), we obtain an expression for tank pressure ratio p/p_a:

$$\rho_a V_T \frac{d}{dt}\left[(p/p_a)(1 - t/t_{fill})\right] = -\frac{[(p/p_a)^2 - 1]^{1/2} A \, p_a}{(RT)^{1/2}[2\ln(p/p_a) + 4f \, L/D]^{1/2}}$$
$$+ K \dot{M}_c \left(\frac{t_{fill}}{t}\right)^{1/2} \tag{11}$$

Differentiating the left hand side and dividing by $\dot{m}_c$, we can derive

$$t_{fill}(1 - t/t_{fill}) \frac{d(p/p_a)}{dt} = p/p_a + K \left(\frac{t_{fill}}{t}\right)^{1/2} - \frac{[(p/p_a)^2 - 1]^{1/2} \sqrt{RT}}{(Q/A)[2\ln(p/p_a) + 4f \, L/D]^{1/2}}$$
$$\tag{12}$$

---

* R is defined as follows: $R = .00232/(\text{molecular weight})$ in units $psi^2\text{-}ft^4\text{-}sec^2\text{-}lbm^{-2}\text{-}°R^{-1}$. The acceleration due to gravity is included in the gas constant to convert lbm/in^2 to psi.

Equation (12) is subject to the initial condition $p/p_a = 1$ at $t = 0$ and can be numerically integrated. The initial problem of $K/\sqrt{t}$ going to ∞ as $t \rightarrow 0$ was overcome by a numerical technique. The key parameters in Equation (12) are $\dot{Q}/A$, K, t_{fill}, and $4f \, L/D$. Values of these parameters were selected from Table II-3 (page 13).

D. Results for Non-Volatile Cargoes $(K = 0)$

In order to compare the pressure time history expected for various vent systems, cargoes, and loading rates, ranges of values of the different cargo transfer parameters were chosen from Table II-3 as follows:

$4f \, L/D$ ratio values = 20, 60, and 200;

$\dot{Q}/A$ values = 10, 30, and 100 ft/sec.

It was found from the results that, for "typical" $\dot{Q}/A$ and $4f \dfrac{L}{D}$ values, the predicted pressure rise is very small. The predicted pressure rise obtained under the conditions $4f \, L/D = 10$ and $\dot{Q}/A = 100$ ft/sec is shown in Figures IV-4 and IV-5. In these figures, the predicted tank pressure rise is plotted against the fraction of total fill time. Also indicated in the figures is the pressure range in which the tank is expected to fail. In Figure IV-4, the pressure is plotted on a log scale to bring out the differences in the predicted pressure values clearly. In Figure IV-5, linear scale plots are used so that the timewise development of the pressure is shown more clearly. In addition, the relative magnitudes of the highest tank pressure achieved and the expected tank failure pressure range are shown.

Table IV-1 shows the maximum pressure as obtained from incompressible flow model* and the compressible adiabatic flow model for different characteristic $\dot{Q}/A$ velocities and $4f \, L/D$ values. It is seen that for several of the cases considered with compressible flow, the Mach Number at the exit section becomes 1, resulting in choked flow conditions. When such a situation results, the calculation procedure programmed on the computer leads to physically impossible solutions (because in the adiabatic calculations, provision is not made for the occurrence of choked flow). These situations are indicated in Table IV-1 with "X" marks.

*The incompressible flow model is the same as equation (12) for $\rho/\rho_a = 1$.

32

Tank Pressure (psig)

100
70
50
30
20

10
7.0
5.0

3.0

2.0

1.0

0.7

0.5

0.3

0.2

0.1

Regime of Expected Tank Failure

$K = 0$

$4\,fL/D = 10$
$\dot{Q}/A = 100$ Ft/Sec

Compressible Flow
No Evaporation

Incompressible Flow

0   .1   .2   .3   .4   .5   .6   .7   .8   .9   1.0
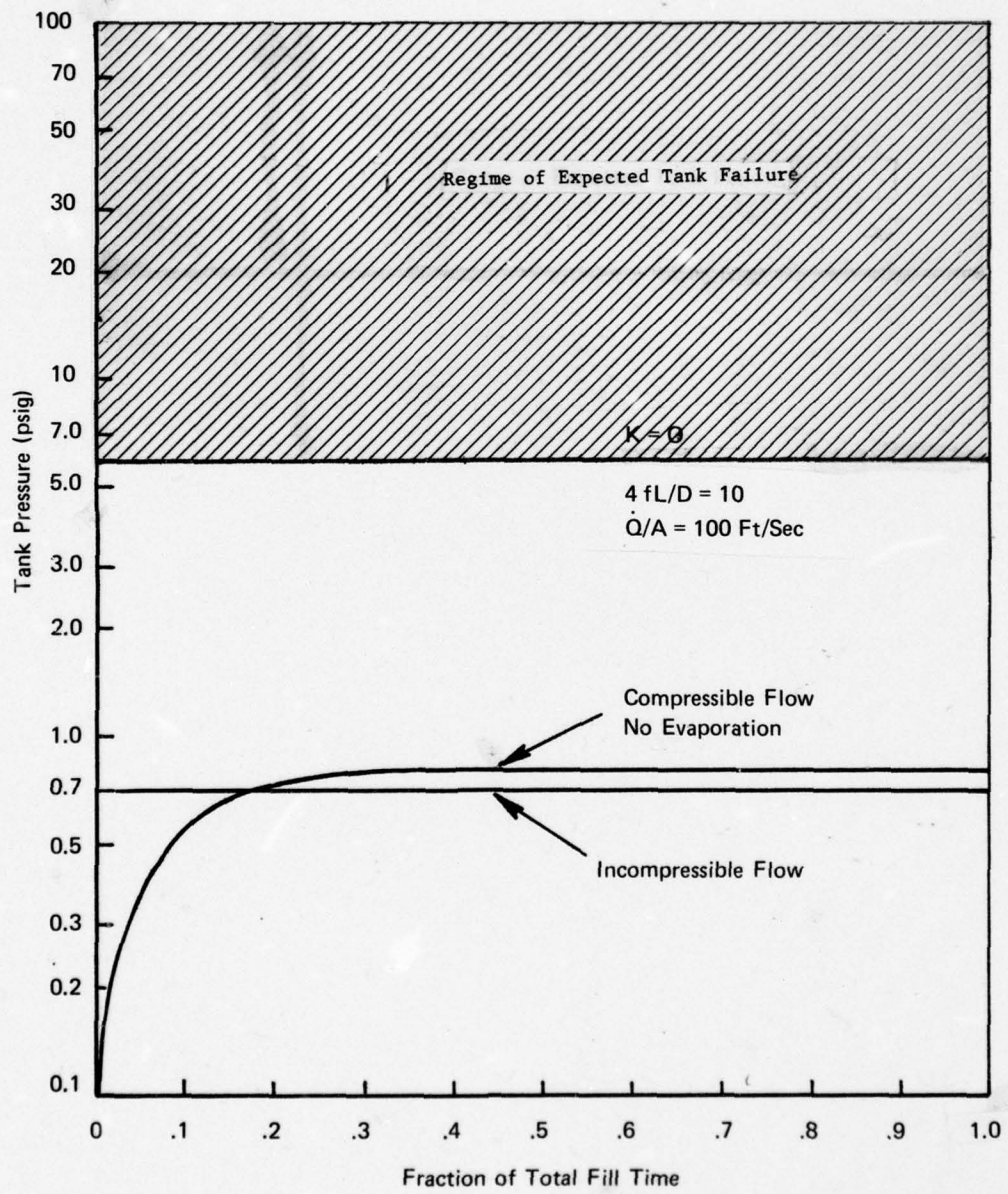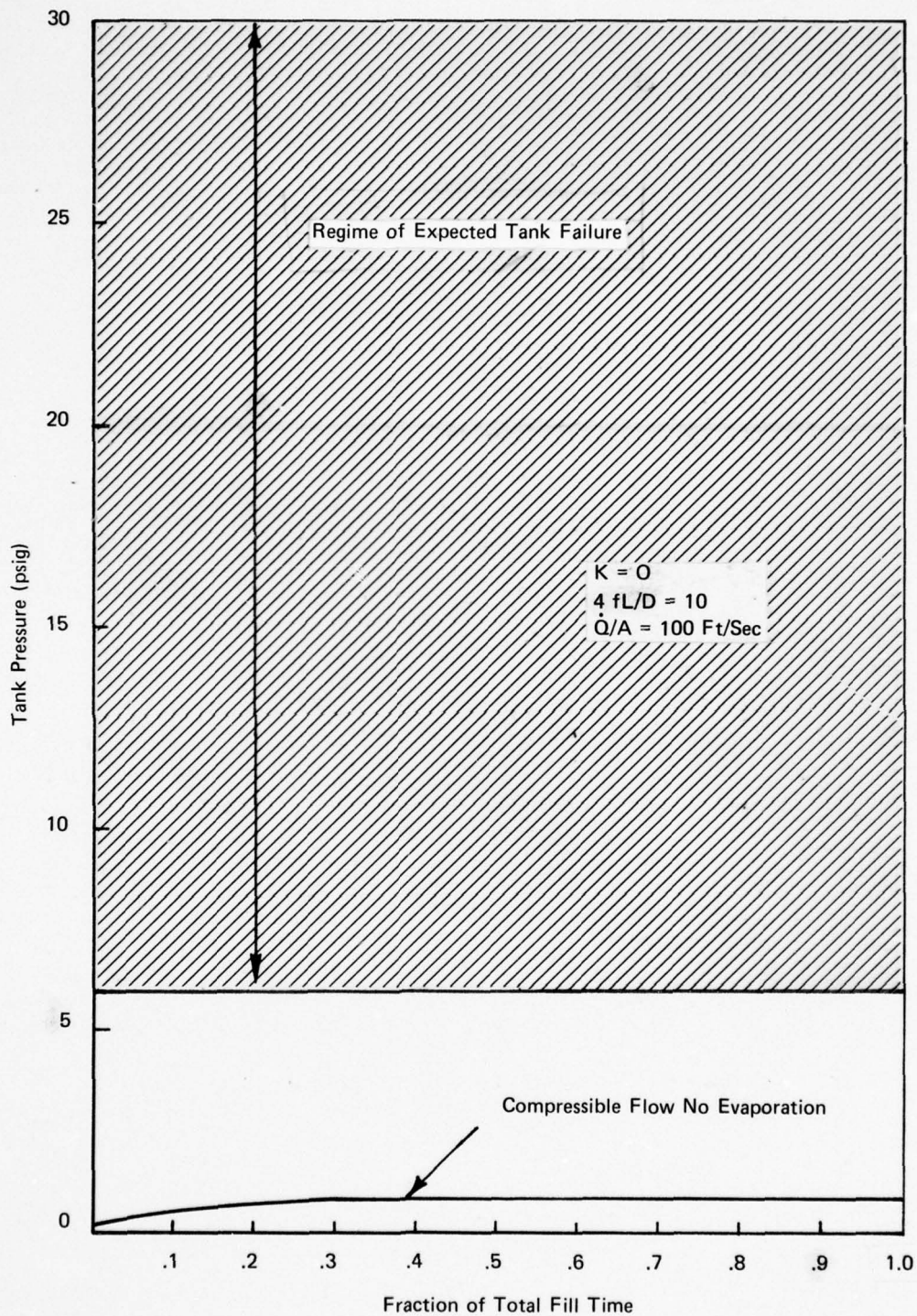
Fraction of Total Fill Time

FIGURE IV—4

FIGURE IV–5

It is seen from Figure IV-4 that there is not a lot of difference in the maximum pressure values from incompressible vs. adiabatic compressible flow. This is understandable because even under the condition of $\dot{Q}$/A = 100 ft/sec, the flow Mach Number is only about 0.1. This indicates that compressibility effects are small.

The second important point noticed from the calculations is that the maximum pressures are far less than the failure pressure of the tank. This indicates that the venting system (even at the high gas flow velocities of 100 ft/sec) is capable of venting all of the gas that is being expelled, with pressure build-up not more than a few psi. It is emphasized that the results hold good only for gas venting and do not extend to liquid venting.

Results shown in Table IV-1 indicate that when either flow velocity is high or friction is high, the back pressure (tank pressure) becomes high and the differences using incompressible and compressible become considerable. For example, for $\dot{Q}$/A = 100 ft/sec and L/D = 3000,* the peak pressure predicted by incompressible methodology gives P_{max} = 4.85 psig, whereas with the compressible methodology, P_{max} = 10.5 psig (which is 2.17 times that given by incompressible theory on gage pressure basis). This indicates that compressibility of gas becomes a very important issue when the frictional resistance in the venting valve-pipe system becomes large. It is, however, comforting to note that for typical shiptank venting systems, (L/D) is of the order of 150 to 500. In such cases, the peak pressure can be predicted very easily using the incompressible equation.

From the analyses and results, we conclude that for non-volatile cargoes (K = 0),

- The peak tank pressures resulting during the venting of gas are small compared to the tank failure pressures.

- The peak pressures can be calculated by a simple incompressible analysis when the gas flow rates in the vent system are small compared to the velocity of sound in the ambient atmosphere.

---

*4f L/D = 60

TABLE IV-1

Effect of Gas Compressibility, Vent Pipe Length, and Gas Flow Velocity on Peak Tank Pressures

Incompressible, No Evaporation

P_{max} (PSIG)

	$\dot{Q}/A$ in ft/sec		
4f L/D	30	100	300
20	0.15	1.62	14.55
60	0.44	4.85	43.66
200	1.46	16.17	145.53

Compressible, No Evaporation

P_{max} (PSIG)

	$\dot{Q}/A$ in ft/sec		
4f L/D	30	100	300
20	0.15	1.94	✕
60	0.46	10.51	✕
200	1.71	✕	✕

- High friction (caused by a constricted vent or extremely long
length of venting pipes) tends to make the peak pressures high.
Under these conditions, the value obtained from simple incom-
pressible analysis is inaccurate.

E. Results for Venting with Cargo Evaporation

1. Magnitude of the Pressure Rise

For normal vent systems, cargo volatility, and loading rates, it
appears that there is about a safety factor of three in tank pressure rise.
For example, we have solved Equation (12) for the case of

- Vent restriction 4f L/D = 20;

- $\dfrac{\text{Loading Rate}}{\text{Vent Area}} = \dot{Q}/A = 30$ ft/sec; and

- $\dfrac{\text{Evap Rate}}{\text{Loading Rate}} = K = 0.5$

For this case the pressure increases rapidly to about 2 psig during the
first 4% of the loading time (approximately 10 minutes). Then as the
evaporation rate falls off, the tank pressure drops to less than 1 psig.
In practice the relief valve would close as the pressure dropped and re-
open only for pressures greater than the set point (2 psig is common).
Comparison of this result to the results in Section D for no evaporation
indicates that evaporation has the effect of increasing the maximum
pressure early in the loading period by about 1 psig. This does not pre-
sent a hazard, but again only holds for normal venting conditions. Let
us examine the individual factors which can lead to higher pressure rise
during abnormal cargo transfer situations.

2. Effect of Vent Restriction

Normally, the vent system restriction (with valves open) corresponds
to an effective L/D of 500 for manifold systems. For f = .005 this cor-
responds to 4f/L/D = 10. Again, this normal extent of vent restriction
gives rise to tank pressures of less than 2 psig. Now if L/D is increased
a factor of 6, the peak pressure goes up to 3.3 psig and is reached at
about 14% of the total fill time, as shown in Figure IV-6. If the ef-
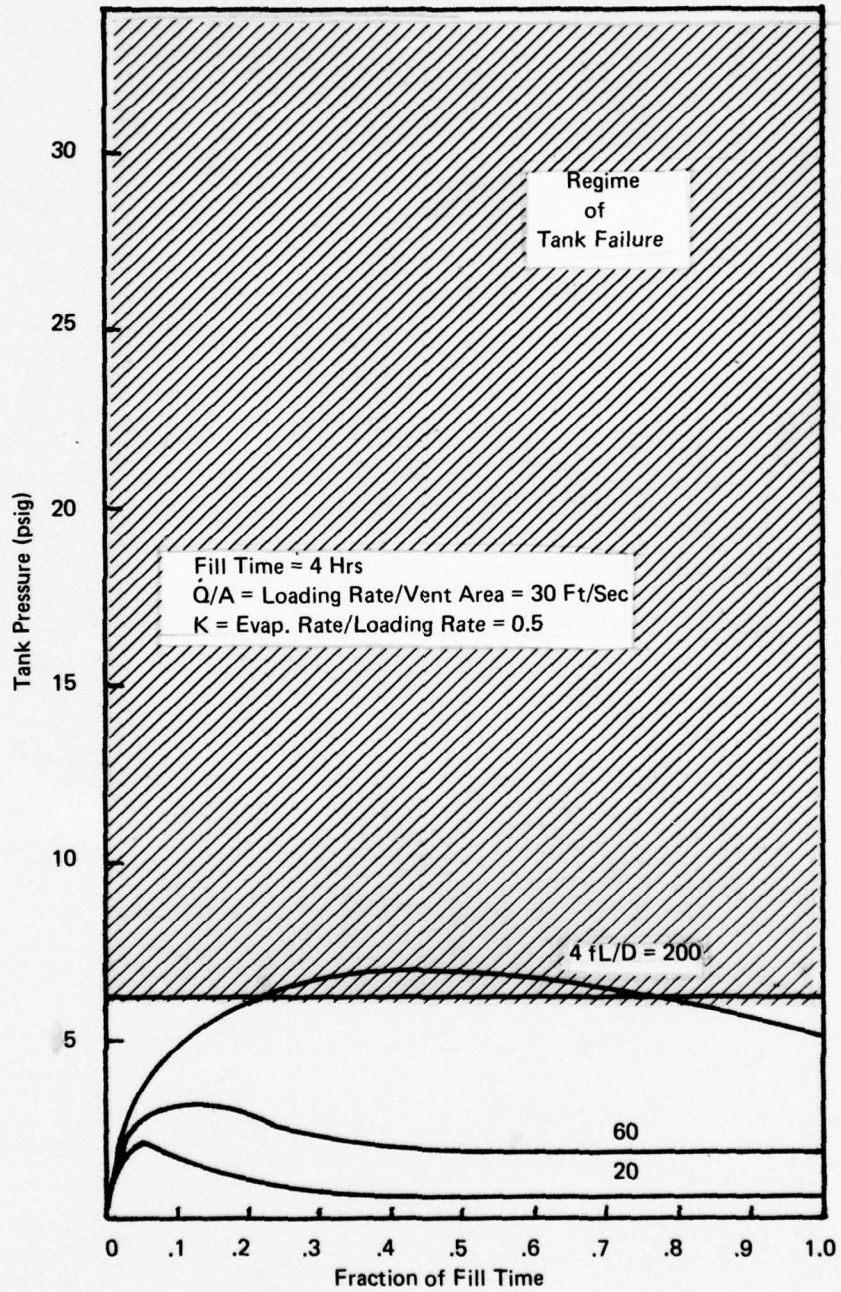fective L/D is increased a factor of 20, say by a blockage or sticky PV

FIGURE IV—6   EFFECT OF VENT RESTRICTION

38

valve, then the maximum pressure is over 7 psig and is stabilized at about 40% of the total fill time. Clearly, tank failure is risked only for restrictions having an effective L/D on the order of 6,000 which is more than ten times normal for a manifold vent system.

3. Effect of Loading Rate and Vent Capacity

The key parameter here is the ratio of loading rate to vent cross sectional area, $\dot{Q}/A$, which has the units of velocity and is normally 10-30 ft/sec. If for some reason the loading rate is increased by a factor of 3.3 (from 30 ft/sec to 100 ft/sec), then the peak pressure would go up from 2 to 6.5 psig, as shown in Figure IV-7. This is on the border of the hazardous range. If the loading rate is ten times normal, or if the vent pipe size is one-tenth the usual area, then the tank pressure goes up steadily and can cause tank failure after less than 10% of the fill time (24 minutes). The $\dot{Q}/A$ and L/D combinations leading to hazardous tank pressures are to be found from Table IV-2.

4. Effect of Cargo Volatility

The effect of cargo volatility manifests itself in the first one-fifth of the cargo transfer operation, as shown in Figure IV-8. Using identical loading rate and vent system, a cargo with a high vapor pressure (K = 0.7) gives rise to a peak tank pressure of 2.6 psig compared to the value of 1.0 psig reached by a less volatile cargo (K = 0.3). Note that these tank pressures are much less than the corresponding equilibrium vapor pressures, implying that diffusion markedly limits the extent of vapor addition.* The tank pressures are well below the hazardous regime above 6 psig, so that it appears that even an extremely volatile cargo (p_{vap} = 14.7 psi at 70°F) would not cause a problem unless $\dot{Q}/A$ or L/D is excessive.

---

*This comment is subject to the assumptions of the evaporation model.

39

Regime
of
Tank Failure

$\dfrac{\text{Loading Rate}}{\text{Vent Area}}$ = 300 Ft/Sec = $\dfrac{\dot{Q}}{A}$

K = Evap. Rate/Loading Rate = 0.5
4 fL/D = 20

100 Ft/Sec

30 Ft/Sec

Tank Pressure (psig)

30

25

20

15

10

5

0   .1   .2   .3   .4   .5   .6   .7   .8   .9   1.0
Fraction of Fill Time
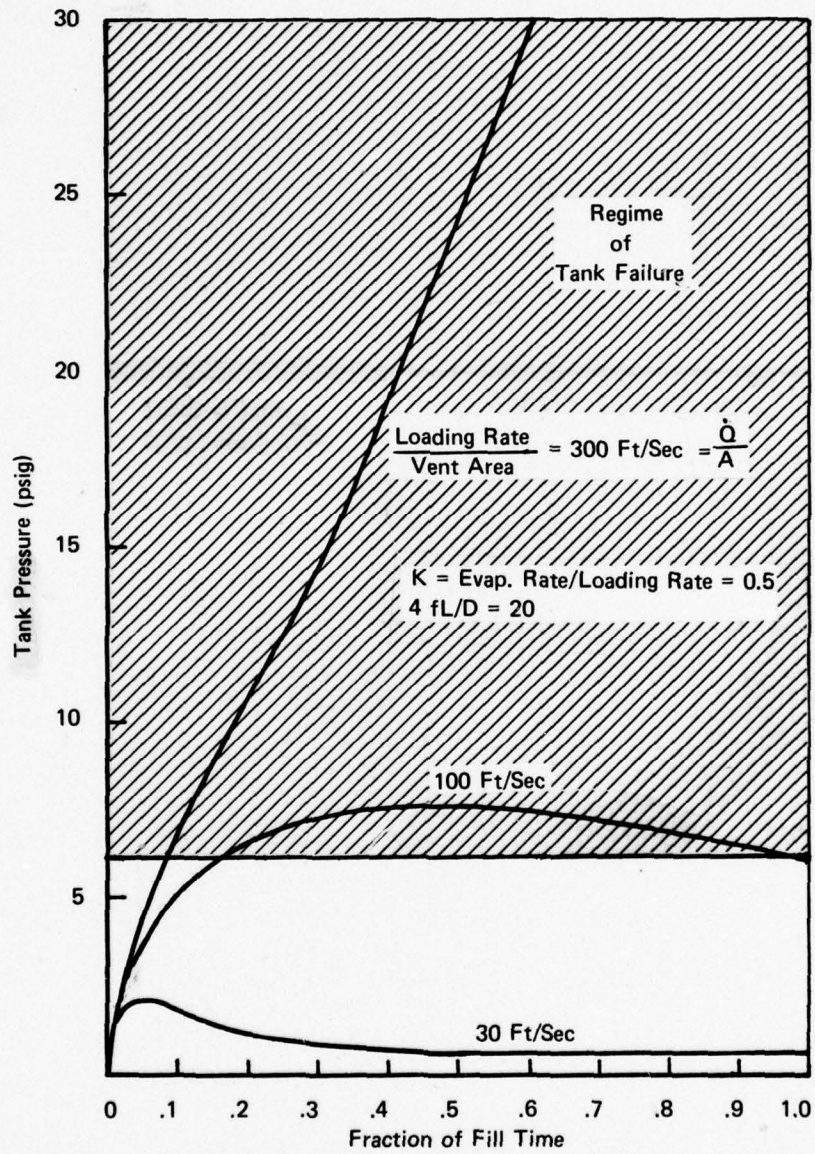
FIGURE IV–7   EFFECT OF LOADING RATE
AND VENT CAPACITY

40

$$\dot{Q}/A \text{ (FT/SEC)}$$

L/D	10	15	20	25	30	40	50	60	80	100	150	200
400							2.7	3.2	4.2	5.3		
600							3.2	3.8	5.1			
800						3.0	3.	4.4	5.9			
1000						3.3	4.1	4.9				
1200					2.8	3.6	4.4	5.4				
1600					3.1	4.1	5.1					
2000				3.0	3.5	4.6	5.8					
2400				3.2	3.8	5.0						
3200			3.0	3.6	4.3	5.9						
4000			3.3	4.0	4.8							
6000	2.2	3.0	4.0	4.9	6.0							
8000	2.5	3.5	4.6	5.8								
10000	2.7	3.8	5.1									
12000	2.9	4.2	5.6									
16000	3.3	4.8										
20000	3.6	5.4										
24000	3.9	6.0										
32000	4.5											
40000	5.1											

Tank pressure less than 3 psi

Tank pressure greater than 6 psi – hazardous for most vessels

TABLE IV-2

Maximum Tank Pressures (PSIG) for
Given Values of Vent System
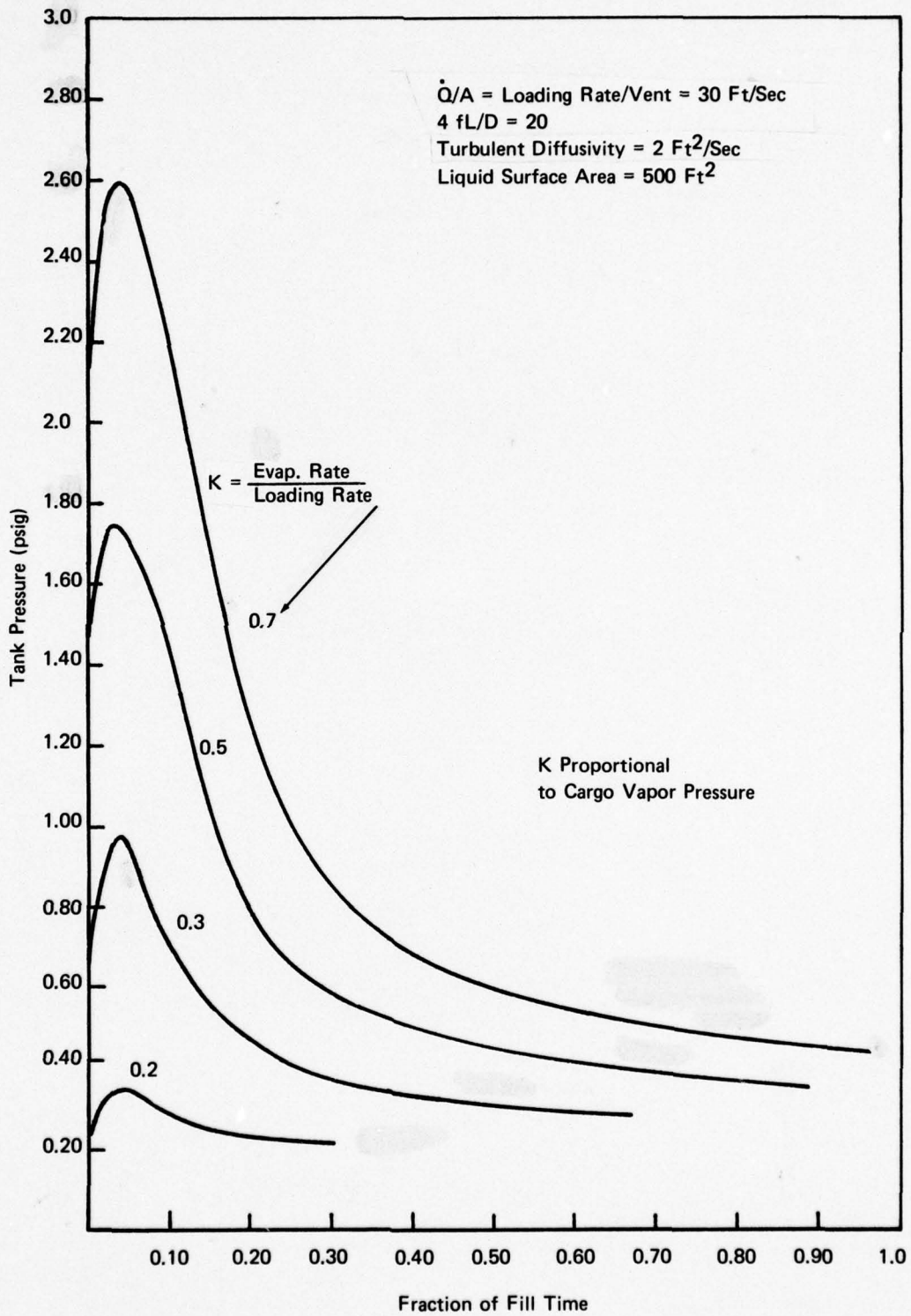L/D and $\dot{Q}/A$ (Based on f = .005)
K ≈ 0.7

FIGURE IV–8   EFFECT OF CARGO VOLATILITY

F. Procedure for Evaluating Overpressure Hazard in an Individual Tank

1. Determine the vent area A (ft^2) from the cross-sectional area of the vent pipe(s) leading from the tank.

2. Determine the loading rate $\dot{Q}$ (ft^2/sec) for the tank in question from the total pumping rate and the number of tanks to be loaded simultaneously.

3. Calculate the quotient $\dot{Q}$/A (ft/sec) which is the characteristic venting velocity.

4. Determine the effective length-to-diameter ratio L/D of the vent system using Table II-2 and the procedure illustrated in Figure II-6.

5. Use Table IV-2 to find the maximum tank pressure to be expected during cargo transfer, using the values of L/D and $\dot{Q}$/A obtained in steps 3 and 4.

6. Compare the expected tank pressure to the failure pressure which may be obtained (1) from a detailed structural analysis of the vessel in question (see Chapter III) or (2) assumed to be 6 psig in lieu of structural data.

V.   TANK PRESSURE HISTORY DURING OVERFILL

A.   Problem Formulation

The objective is to predict the tank pressure history when the tank is overfilled while being loaded with liquid cargo. The physical system to be modeled is shown in Figure V-1. At the point at which the tank is full, the pumping process will begin to displace liquid into the vent system. This causes a pressure drop due to friction and due to the vertical head of the liquid in the vent piping. The system attempts to relieve this pressure drop in two ways: (a) by compressing the liquid, and (b) by expansion of tank walls.

In the present analysis, the tank pressure is defined as the pressure in the liquid at the top part of the tank. As shown in Figure V-2, the pressure at the top of the tank is less than the pressure at the bottom of the tank because of the liquid head.

Additional Pressure Drop
From Fittings

Friction

Vertical Head

Tank Walls Expand

Liquid
Compresses

t = 0
Cargo Fills Tank

t = 1 - 10 sec.
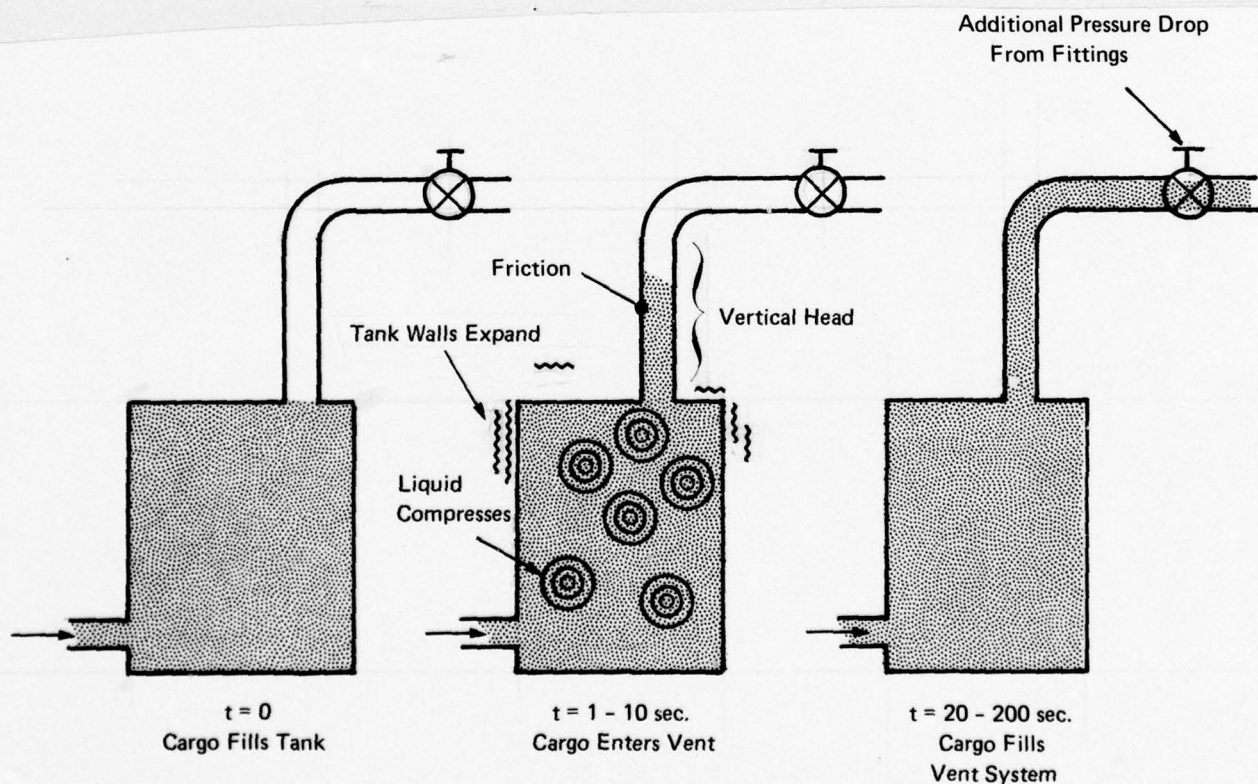Cargo Enters Vent

t = 20 - 200 sec.
Cargo Fills
Vent System

FIGURE V-1   SCHEMATIC OF THE PHYSICAL SYSTEM FOR
MODELING THE TANK PRESSURE RISE
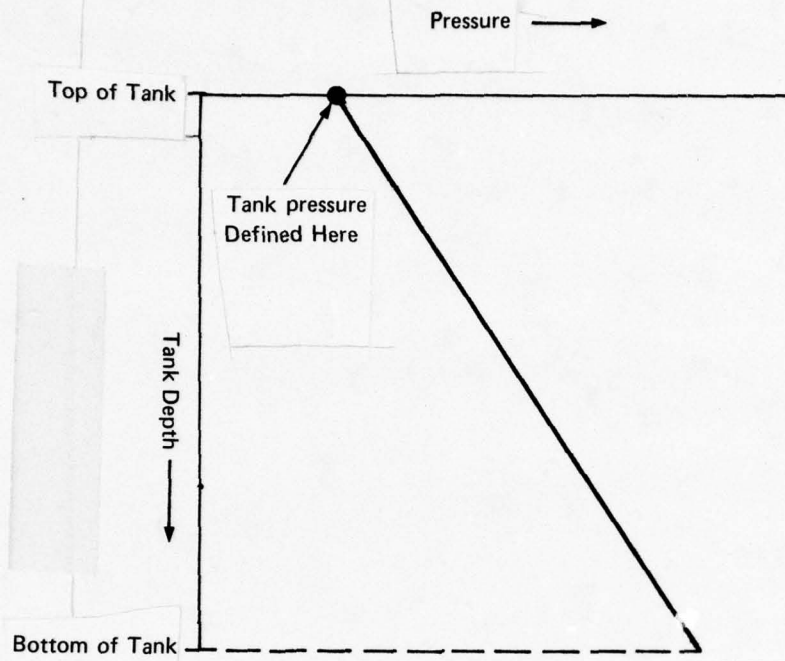
**FIGURE V—2   VERTICAL PRESSURE GRADIENT
DUE TO HYDROSTATIC HEAD**

B. Analysis

We first write a mass balance for the tank-liquid system. Then the
rate of mass outflow (exit velocity) and the rate of mass accumulation
within the tank are related to the tank pressure. This results in an
equation describing the time rate of increase of pressure, which is
solved numerically to obtain tank pressure as a function of time. These
steps are shown below.

$$\frac{dM}{dt} \quad = \quad \dot{M}_i \quad - \quad \rho AU \tag{13}$$

| Rate of accumulation of mass within the tank | Inlet mass flow rate of liquid | Outflow rate of liquid from the tank |

Here we take U to be the average liquid velocity in the vent system at any instant. The rate of accumulation of mass is related to the rate of pressure rise through equation (18), which is derived as follows:

$$M = \rho V_T \tag{14}$$

where V_T is the tank volume.

Differentiating equation (14) with respect to time, we get

$$\frac{dM}{dt} = \rho \frac{dV_T}{dt} + V_T \frac{d\rho}{dt} \tag{15}$$

For constant temperature, we have

$$\left. \begin{array}{l} V_T \equiv V_T(p) \\ \rho \equiv \rho(p) \end{array} \right\} \tag{16}$$

Therefore,

$$\frac{dM}{dt} = \frac{dp}{dt} \left[\rho \frac{dV_T}{dp} + V_T \frac{d\rho}{dp} \right] = \rho V_T \frac{dp}{dt} \left[\frac{1}{V_T} \frac{dV_T}{dp} + \frac{1}{\rho} \frac{d\rho}{dp} \right] \tag{17}$$

Using the definitions of compressibility and the volumetric expansion coefficient (see nomenclature), we have:

$$\frac{dM}{dt} = M[\beta + \kappa] \frac{dp}{dt} \tag{18}$$

Substituting equation (18) into equation (13), we get

$$\frac{dp}{dt} = \frac{1}{(\beta + \kappa)} \left[\frac{\dot{M}_i - \rho A U}{M} \right] \tag{19}$$

The mass in the tank M is given by

$$M = M(0) + \int_0^t (\dot{M}_i - \rho A U) \, dt \tag{20}$$

Hence, equation (19) can be written, after substituting for M from equation (20) and dividing both numerator and demoninator by ρA, as

$$\frac{dp}{dt} = \frac{1}{(\beta + \kappa)} \left[\frac{(\dot{Q}/A) - U}{(V_T/A) + (\dot{Q}/A) \ t - \int_{o}^{t} U \ dt} \right] \qquad (21)$$

Before we can solve equation (21), we will need to relate the outflow velocity U with the tank pressure p.

The above equation is the fundamental equation for estimating the pressure in the tank as a function of time. Depending on the assumptions for U (p), β, and κ, the rate of rise of pressure will be different.

The following assumptions and effects are reasonable for typical cargoes and vent system designs:

1. Constant mass inflow rate $\dot{M}_i$. The change in liquid density due to compression has a negligible effect on the loading rate (for example, the change in the density of Hexane is 0.04% for every atmosphere change in pressure).

2. Constant κ value.

3. Expansion of the tank due to the internal pressure taken into account by a linear expression (constant value of β).

4. The flow in the vent pipe is fully turbulent (Re > 3000) and therefore the friction factor is a constant.

5. Increased pressure drop occurs as the length of liquid wetting the pipe increases.

6. A sudden increase in pressure drop occurs due to the flow resistance through the valve and/or flame arrestor.

The pressure drop across the vent system will be due to both vertical head of liquid and frictional drop. Therefore, the vent system must be described before deriving Δp. The vent system is assumed to consist of a vertical pipe section of height H followed by a horizontal (or near horizontal) section ending in a P-V valve and a flame arrestor, as shown in Figure V-3. The total geometric length of the pipe equals L_1. The total effective length, including valves and fittings, is L.
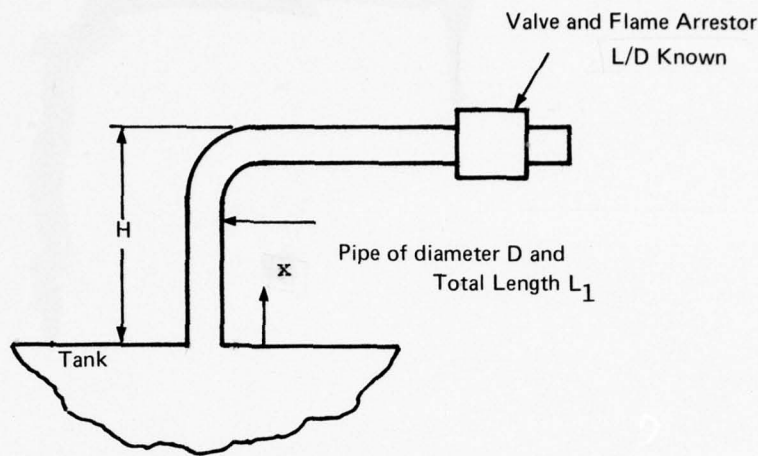
47

FIGURE V—3   SCHEMATIC DIAGRAM OF THE VENT SYSTEM

The tank pressure is related to mass outflow velocity through the vent system
by the expression

$$p = p_a + \rho\, g\, x + \frac{1}{2}\,(4f)\,\frac{y}{D}\,\rho\, U^2 \tag{22}$$

where x is the vertical column of the liquid in the vent pipe ($x \le H$)
and y = total length of liquid wetted pipe at any instant ($y < L_1$).
In using Equation (22), the reader is cautioned to divide the second and
third term by 144 in order to convert lbm/ft^2 to psi which appears through-
out the text.

When $y = L_1$, liquid has completely filled up the pipe and is venting
out to the atmosphere. Under this situation, the length y which appears
in the last term of equation (22) becomes L, the effective length of
the vent passage, including the equivalent length of valves and fittings.
Thus, the definitions needed to supplement equation (22) are as follows:

$$x = \begin{cases} y \text{ for } y < H \\ H \text{ for } y > H \end{cases} \tag{23}$$

$$y = \begin{cases} \displaystyle\int_0^t U \, dt & \text{for } y < L_1 \\[12pt] L & \text{otherwise} \end{cases} \tag{24}$$

Equations (21) and (22) form a coupled set of two nonlinear equations for two unknowns, U and p. It is also necessary to use equations (23) and (24) in the solution.

The initial conditions are given by

$p = p_0$ at $t = 0$ where p_0 is given by solving equation (12) at
$\qquad t = t_{fill}$ for gas venting. $\tag{25}$
$U = U_0$ at $t = 0$

The iterative solution procedure for obtaining p and U as functions of time is shown in Appendix C. The results for specific tank conditions are discussed in a later section. The initial condition for vent exit velocity is derived in Appendix D. The key parameters in the solution are κ, β, H, $\dot{Q}/A$, and 4f L/D.

C. Determination of Parameters

Suppose a tank 17 ft wide by 40 ft long by 90 ft deep is being filled with hexane. The vent pipe is 4 inches in diameter and 50 ft long and has a vertical section which is 10 ft in length. The liquid filling rate is such that the entire tank fills up in four hours. The equivalent (L/D) ratio for friction through the valve is 100. The data for a chemical tanker needed to derive the coefficients for equations (21) - (25) are as follows:

- Volume of tank = V_T = 61200 ft^3

- Tank filling time = $V_T/\dot{Q}$ = 4 hours

- Inflow rate (volumetric) = $\dot{Q}$ = 4.25 ft^3/s

- Total length of vent pipe = L_1 = 50 ft

- Diameter of vent pipe = D = 1/3 ft

- Equivalent (L/D) for valve = $(L/D)_{valve}$ = 100

- Volumetric expansion coefficient for the tank = $\beta = 1.7 \times 10^{-3}$/atm (see Appendix E)

- Coefficient of friction for flow in vent pipe = 4f = 0.01

49

- Liquid used in the tank = Hexane

- Density at ambient pressure and temperature = ρ_o = 41.12 lbm/ft^3

- Compressibility = κ = 2.75 x 10^{-5} psi^{-1}
  (see Handbook of Physics and Chemistry, page 209, Table 165)

The initial flow velocity (at zero time) of liquid into the vent pipe is calculated using the procedure illustrated in Appendix D. The value obtained for the above values of the parameters is

U_o = 1.6 ft/sec.

Arthur D. Little, Inc.

D. Results and Discussions

1. Hazardous Loading Conditions

The liquid efflux velocity U which corresponds to a hazardous 6 psig tank pressure can be obtained from Equation (22):

$$U = \left(\frac{p - p_a - \rho g H}{\frac{1}{2} \rho \, 4f \, L/D} \right)^{1/2}$$

Substituting 4f L/D = 10 and H = 8 ft for a normal manifolded vent system, we obtain U = 9 ft/sec. If $\dot{Q}/A$ is less than approximately 9 ft/sec, pressures approaching those necessary to rupture the tank would not be expected. Liquid cargo can pass through the vent system indefinitely only if the vent capacity and loading rate are such that U is well below this value.

For higher loading rates or smaller vent capacities, tank failure appears to be inevitable. The pertinent question is how much time does the operator have to react to an overfill condition. We have conducted a numerical analysis for two cases in this failure regime:

      o   Loading rate/vent area = $\dot{Q}/A$ = 49 ft/sec; and

      o   Loading rate/vent area = $\dot{Q}/A$ = 98 ft/sec.

The results of the numerical integration of Equations (21) and (22) are shown in Figures V-4 and V-5. The tank (top) pressure is plotted as a function of dimensionless time. Figure V-4 is for a four-hour fill time and V-5 for a two-hour fill time. Results for three values of the coefficient 4f L/D appear on each Figure: 10, 100, and ∞ (blocked vent). From Table II-3 it can be seen that typical vent systems are in the range 3 < 4f L/D < 10.

2. Effect of Vent L/D, Cargo Viscosity, and Vertical Runs

It is seen from Figures V-4 and V-5 that most of the pressure rise is due to the friction generated by flow in the vent. The effect of hydrostatic head is negligible (hydrostatic pressure due to 10 feet of vertical pipe with Hexane is approximately 3 psig).

51

3. Effect of Tank Expansion

The flow velocity in the vent is very small in the beginning compared to the 98 ft/sec characteristic velocity $(\dot{Q}/A)$, expected for an inviscid fluid. Even when the total pressure drop has increased to 2 atm the mean flow velocity is still only about 25% of characteristic velocity. This indicates that there is considerable accumulation of liquid in the tank due to tank flexing.

4. Effect of Loading Rate

Comparison of Figure V-4 vs. Figure V-5 shows that the rate of pressure rise is higher when the liquid inflow rate is higher. If the inflow rate is doubled, a given tank pressure is reached in about half the time (time being counted after the tank is full of liquid).

5. Magnitude of Pressure Rise

From the results shown in Figure V-5, it is seen that for a two-hour fill time (which is an excessive rate according to Table II-3), the tank pressure reaches 10 psig in about 10 seconds and continues to increase. Thus, tank failure is expected in a very short interval for an overfill at high loading rates.

For a loading rate on the high end of the "normal" range (4-hr time; see Figure V-4), the pressure reaches 10 psig in about 30 seconds.

Calculations were repeated on the assumption that the vent is blocked. The following equation is obtained from Equation (21) by substituting $U = 0$:

$$p - p_a = \frac{1}{(\beta + \kappa)} \, \ln \left(1 + \frac{\dot{M}_i}{M(0)} \, t\right) \qquad (26)$$

Using the above formula with appropriate values for the parameters, it is seen that for a tank being filled with liquid in two hours, the time to reach 6 psig is between 3 and 10 seconds which agrees closely with the case of $4f \, (L/D) = 10$. Further results of calculations with the assumption of blocked vent after the tank is completely liquid full are shown in Table V-2.

Table V-2

Tank Pressure as a Function of Time
When the Vent is Blocked
(Two Hour Tank Fill Time)

Time (Seconds)	Pressure (psig)
0.5	0.44
1.0	1.03
1.5	1.47
2.0	1.91
2.5	2.35
3.0	2.94
10	9.7
50	48.1
100	95.84
200	190.37

The above comparison indicates that for these calculations, the blocked vent result will give a reasonably close (and certainly a conservative) estimate of the time of bursting of the tank shell.

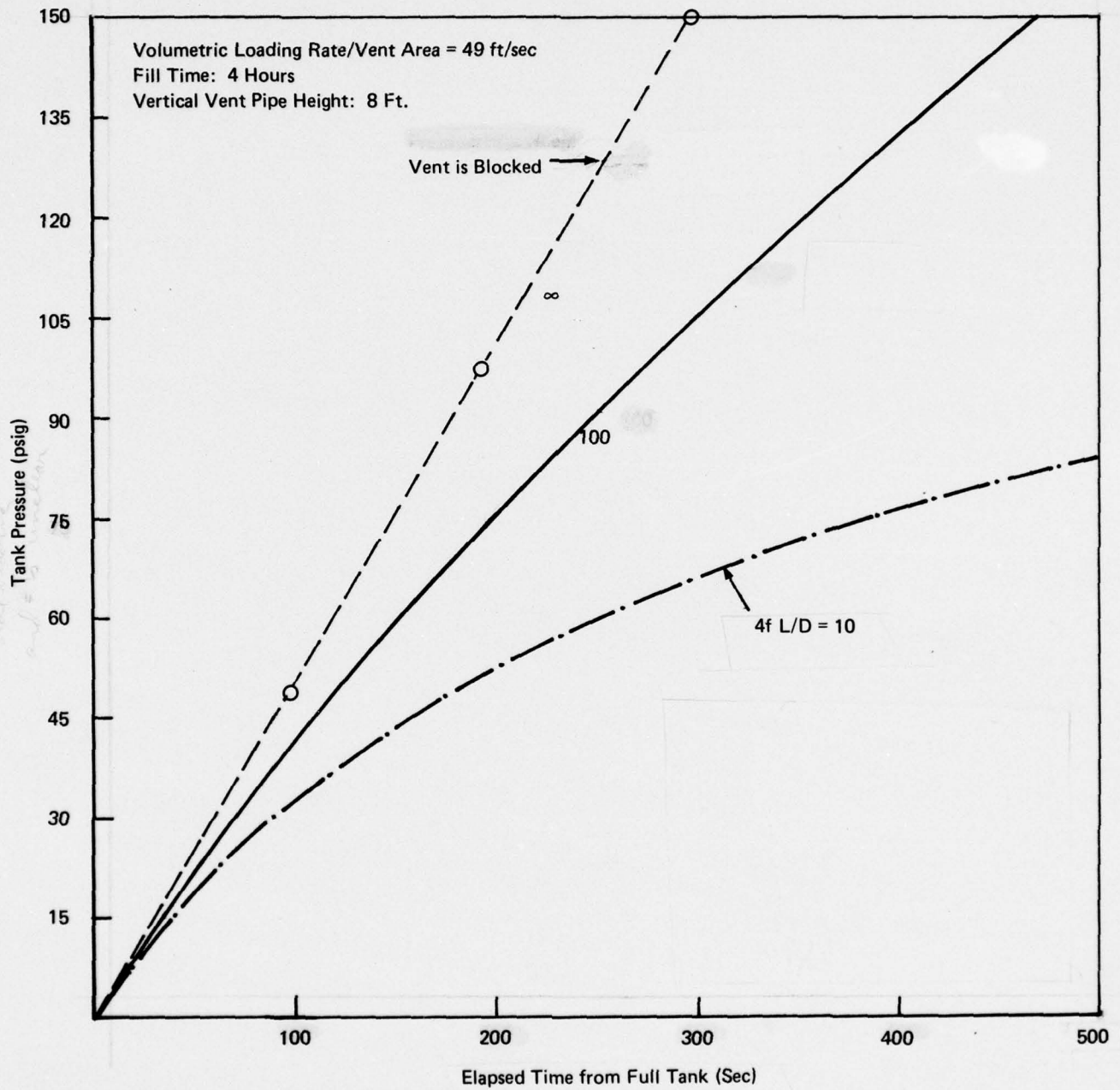**FIGURE V–4 PREDICTED TANK PRESSURE DURING OVERFILL (EXCESSIVE LOADING RATE)**

Volumetric Loading Rate/Vent Area = 98 ft/sec
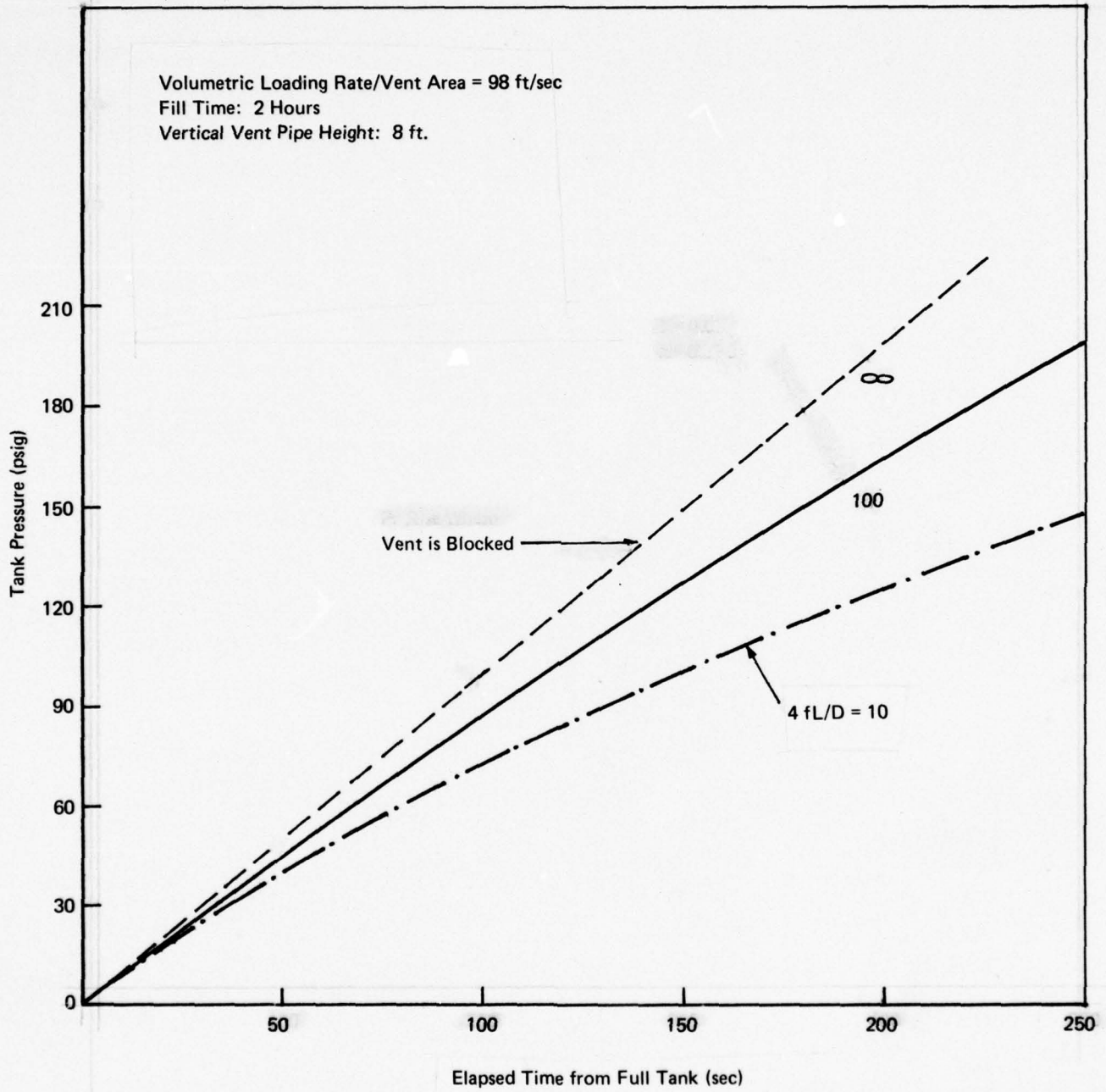Fill Time: 2 Hours
Vertical Vent Pipe Height: 8 ft.

FIGURE V–5   PREDICTED TANK PRESSURE DURING
OVERFILL (HIGH LOADING RATE)

E. Summary of Findings and Measures to Avoid Overfill

Mathematical models have been developed to obtain the rise in the tank pressure of a tank when it starts venting liquid after attaining the liquid full condition. It is assumed in these models that there is a constant inflow (rate) of liquid maintained. The models take into consideration the volumetric expansion of tanks, the flow friction in the vent, and the pressure drop of the valves in the vent and hydrostatic heads due to the vertical sections of the vent pipe.

The procedure for determining if a given loading rate and vent system will present an overpressure hazard for an individual tank upon overfill is as follows:

1. Determine the venting area A (ft^2) from the cross sectional area of the vent pipe(s) loading from the tank.

2. Determine the loading rate $\dot{Q}$ (ft^3/sec) for the specific tank from the total pumping rate and the number of tanks to be loaded simultaneously.

3. Calculate the quotient $\dot{Q}/A$ (ft/sec) which is the characteristic venting velocity.

4. Determine the effective length to diameter ratio L/D of the vent system using Table II-2 and the procedure illustrated in Figure II-6.

5. Use Equation (22) to find the maximum tank pressure to be expected during cargo overfill, using the values of $\dot{Q}/A = U$ and L/D = y/D obtained in steps (3) and (4), respectively.

It is seen from our results that when the loading rate is excessive for the vent capacity, the burst pressure of the tank is reached in a relatively short time after the tank goes liquid full. Tank damage can be avoided by an automatic shut-off mechanism which detects (a) the liquid level in the tank or (b) the rapid pressure rise, and quickly shuts off the inflow of liquid to the tank. Method (b) could lead to line rupture, however. Alternatively, overfill tanks and spill valves can be provided. Prevention of liquid overfill condition is imperative to protect the tank.

The pressure time history in the initial stages can be predicted with reasonable accuracy by assuming the vent to be completely blocked off.

56

Arthur D Little Inc

Tank flexure plays an important safety role in relieving overfill pressure. If the tank is infinitely rigid, the rate of pressure rise in the tank is extremely rapid, and burst pressure will be attained within a fraction of a second. Our calculations show that the delay times between filling the tank and reaching burst pressure are very short (less than 30 seconds).

Preventative measures would include flow metering devices to alert the operator of excessive loading rates, continuous guaging systems based on liquid level sensors with high level alarms, remote actuated quick closing valves, and spill valves.

NOMENCLATURE

		Units
A	= cross sectional flow area	ft^2
c	= velocity of sound in air at ambient conditions	ft/sec
D	= inside diameter of vent pipe	ft
E	= modulus of elasticity	psi
f	= fanning friction factor in the vent pipe	-
f_e	= effective friction factor 2 f L/D	-
g	= acceleration due to gravity	ft/sec^2
h	= thickness of bulkhead panel	in
H	= height of the vertical portion of the vent pipe	ft
I	= moment of inertia of panel or beam section	in^4
K	= ratio of evaporation rate to the loading rate, taken at time t_{fill}	-
ℓ	= length of bulkhead panel	in
L_1	= geometric length of vent pipe	ft
L	= effective length of vent pipe	ft
L/D	= effective length to diameter ratio	-
L/D_{pipe}	= length to diameter ratio of the vent pipe	-
L/D_{valve}	= equivalent length to diameter ratio of the valve	-
m	= dimensionless mass of gas in the tank M/M(0)	-
$\dot{M}_v$	= rate of mass efflux through the vent	lbm/sec
$\dot{M}_c$	= characteristic mass efflux rate of air = $\rho_a \dot{Q}$	lb/sec

58

$\dot{M}_{vap}$ = rate of vapor mass addition to the ullage by evaporation lbm/sec

M = mass of liquid in the tank at any time lbm

$M(0)$ = mass of liquid in the tank at the start of overfill lbm

$\dot{M}_i$ = rate of mass inflow (liquid filling rate) lbm/sec

p = pressure inside the tank (at the top of the tank) psi

p_a = atmospheric pressure psi

p_{vap} = equilibrium vapor pressure psi

P = gauge pressure inside the tank psig

ρ = (p/p_a) = dimensionless pressure –

P_D = dimensionless hydrostatic head due to a diameter high column of liquid in the vent pipe –

$\bar{P}$ = dimensionless gauge pressure inside the tank psig

$\dot{Q}$ = volumetric liquid filling rate ft^3/sec

R = gas constant = .00232/molecular weight $psi^2-ft^4-sec^2/°R/lbm^2$

Re = Reynolds number for flow in the pipe = $\dfrac{UD}{\nu}$ –

s = stringer spacing or width of bulkhead panel in

S = surface area of cargo liquid ft^2

t = time sec

t_{fill} = characteristic tank filling time (volume of tank divided by loading rate) sec

t_c = characteristic vent pipe filling time (Chapter V) sec

T = temperature °R

U = mean velocity of liquid in the vent pipe ft/sec

U_o = mean velocity of liquid in the vent pipe at the start of overflow ft/sec

U_c	= mean velocity of the liquid in the vent pipe if the outflow rate is equal to inflow rate	ft/sec
V	= tank volume not occupied by liquid at any instant of time	ft^3
V_T	= total tank volume	ft^3
v	= U/U_c = dimensionless velocity in the vent pipe	-
W	= load	lb
x	= height of the free liquid surface (in the vent pipe) above the tank top when the vent pipe is being filled up	ft
y	= total length of the wetted section of the vent pipe when the vent pipe is being filled with liquid	ft
α_c	= characteristic Mach number	-
α	= Mach number = fluid velocity/local sonic velocity	-
β	= coefficient of volume expansion of tank by pressure $= \frac{1}{V_T}\left(\frac{dV}{dp}\right)$	psi^{-1}
γ	= ratio of specific heats of the gas	-
ϵ	= turbulent diffusion coefficient	ft^2/sec
κ	= compressibility of liquid $= \frac{1}{\rho}\frac{d\rho}{dp}$	psi^{-1}
λ	$= \frac{1}{2} \times 4f \frac{\rho U^2}{p_a}$ = dimensionless pressure drop in a length of vent pipe equal to its diameter	-
ν	= kinematic viscosity	ft^2/sec
ξ	= y/L	-
ρ	= density of liquid	lbm/ft^3
ρ_a	= density of gas	lbm/ft^3
ρ_{vap}	= density of pure vapor	lbm/ft^3

60

τ $\qquad$ $= t/t_c$ = dimensionless time $\qquad$ —

τ_{fill} $\qquad$ $= t_{fill}/t_c$ = dimensionless fill time $\qquad$ —

Subscripts

c $\qquad$ = characteristic value

e $\qquad$ = exit condition

liq $\qquad$ = liquid

vap $\qquad$ = vapor

o $\qquad$ = initial value

τ $\qquad$ = iteration at time τ (Appendix C)

max $\qquad$ = maximum (at the failure limit)

t $\qquad$ = throat

T $\qquad$ = total

REFERENCES

1. American Bureau of Shipping, <u>Rules for Building and Classing Steel Vessels</u>, R. R. Donnelley & Sons Company, Chicago, (1972), <u>Rules for Building and Classing Steel Barges for Offshore Service</u>, (1967), and <u>River Rules</u>, (1971).

2. Baumeister, (Editor), <u>Marks' Handbook for Mechanical Engineers</u>, 7th Edition, McGraw-Hill, New York, (1967).

3. Bird, R. Bryon, et al., <u>Transport Phenomena</u>, Department of Chemical Engineering, University of Wisconsin, Madison, Wisconsin, John Wiley & Sons, Inc., New York, (1966).

4. Bleich, "Buckling Strength of Metal Structures", McGraw-Hill.

5. Clarkson, J., <u>The Elastic Analysis of Flat Grillage</u>, Cambridge University Press, (1965).

6. Farrell, T. R., "Chemical Tankers - The Quiet Evolution", Royal Institution of Naval Architects, Great Britain, (1974).

7. Harrington, Roy L., <u>Marine Engineering</u>, The Society of Naval Architects and Marine Engineers, New York, (1971).

8. Lekhnitskii, S. G., <u>Anisotropic Plates</u>, translated by S. W. Tsai and T. Cheron, Gordon and Breach, New York, (1968).

9. Martin, W. S., "A New Approach to Gas Venting of Tankers", Trans RINA <u>112</u>, (1970).

10. National Academy of Sciences, <u>Pressure Relieving Systems for Marine Cargo Bulk Liquid Containers</u>, Washington, DC, (1973).

11. National Transportation Safety Board, "Explosion and Fire on Board the Unmanned Tank Barge Ocean 80 at Carteret, New Jersey on 25 October 1972 without Loss of Life", U. S. Coast Guard, Washington, DC, (1975).

12. Paterson, I. W. F., et al., "Pressure and Vacuum Relief Systems for Tankers", Northeast Coast Institution of Engineers and Shipbuilders, Great Britain, (1974).

13. Schade, H. A., "The Orthogonally Stiffened Plate Under Uniform Lateral Load", Journal of Applied Mechanics, V7, No. 4, pp. A143 - 146, (1940).

14. Shapiro, A. H., <u>The Dynamics and Thermodynamics of Compressible Fluid Flow</u>, Vol. I, p. 83 ff, Ronald Press, New York, (1953).

15. Wah, Thein, "A Guide for the Analysis of Ship Structures", National Academy of Sciences - National Research Council, Washington, DC.

Appendix A

Alternate Model for Adiabatic Venting

For high loading rates with the standpipe vent system or other situations where the gas residence time in the vent is small, the heat exchange between the vented gas and the ambient may be negligible. In these cases, the appropriate venting assumption is <u>adiabatic</u> rather than isothermal. In order to consider adiabatic compressible flow with friction, the venting system may be considered to be a converging nozzle with a long duct attached as shown in Figure A-1. Shapiro[14] has developed expressions for obtaining the flow mach numbers and the mass flow through such a nozzle-duct system with friction. These expressions are utilized to obtain the mass flow rate through the tank venting system for a given tank pressure. Using this mass flow rate and equation (11), the pressure-time history can be determined. These steps are illustrated below.

Assuming that the friction factor is a constant and using equations developed by Shapiro[14] [Eq. 6.20 and 6.21, page 167], we can relate the throat Mach number (α_t) to the exit Mach number (α_e) through the following expression:

$$2 \, f_e = \frac{1}{\gamma} \left[\frac{1}{\alpha_t^2} - \frac{1}{\alpha_e^2} \right] + \left(\frac{\gamma + 1}{2\gamma} \right) \ln \left[\frac{\alpha_t^2}{\alpha_e^2} \frac{(1 + \frac{\gamma - 1}{2} \alpha_e^2)}{(1 + \frac{\gamma - 1}{2} \alpha_t^2)} \right], \qquad \text{(A-1)}$$

Where we have defined $f_e = \frac{1}{2} (4f \, L/D)$ as the friction parameter.

A-1

Similarly, using equations 6.22 and 4.14-b of Shapiro we can obtain an expression for the pressure ratio in terms of α_e and α_t:

$$\Phi = \frac{p}{p_a} = \left[1 + \frac{\gamma - 1}{2}\,\alpha_t^{\,2}\right]^{\frac{\gamma}{\gamma - 1}} \left[\left(\frac{\alpha_e}{\alpha_t}\right)^2 \frac{\left(1 + \frac{\gamma - 1}{2}\,\alpha_e^{\,2}\right)}{\left(1 + \frac{\gamma - 1}{2}\,\alpha_t^{\,2}\right)}\right]^{1/2}, \qquad (A-2)$$

where α_t and α_e are respectively the local mach numbers at the throat and at the exit section. The mass flow rate can be obtained from Equations (4.11) and (4.14-b) of Shapiro[14] and is given by the <u>Nozzle Mass Flow Equation</u>.
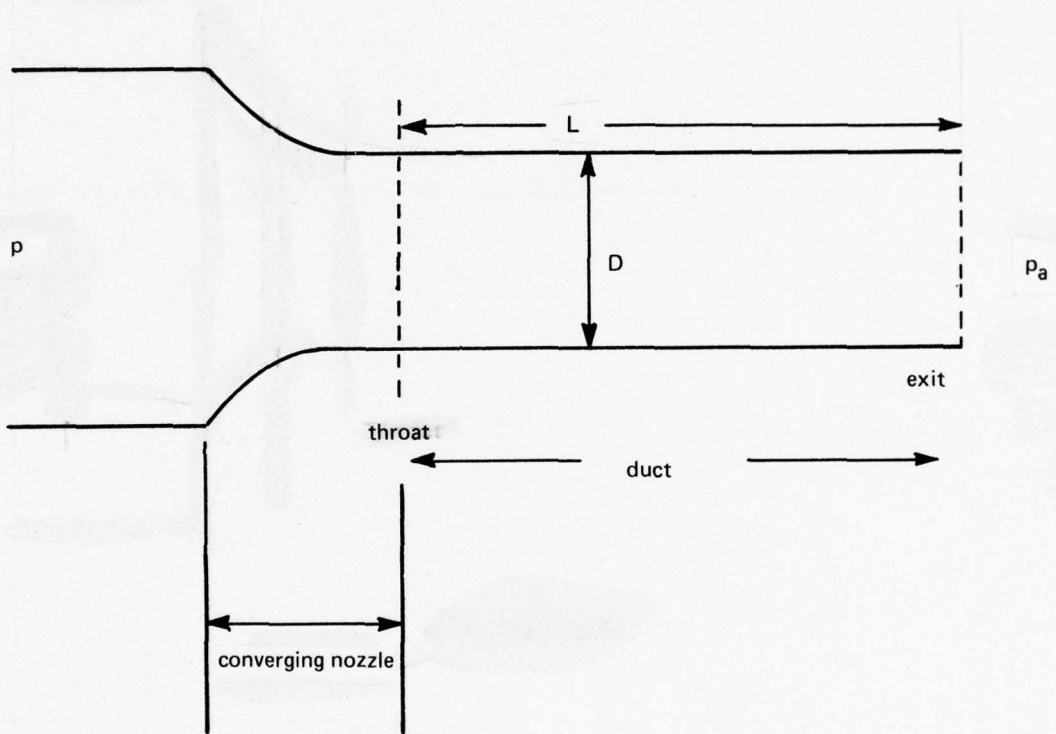
$$\frac{\dot{M}_v}{Ap}\,\sqrt{RT} = \left[\frac{\gamma\,\alpha_t^{\,2}}{\left[1 + \left(\frac{\gamma - 1}{2}\right)\alpha_t^{\,2}\right]^{\frac{\gamma + 1}{\gamma - 1}}}\right]^{1/2} \qquad (A-3)$$

where p and T are respectively the absolute tank pressure and tank gas temperature.

Writing $\dot{M}_v$ in Equation (A-3) in dimensionless form to conform to the definitions of $\dot{m}$ and α_c in the nomenclature, we obtain

$$\dot{m} = \frac{\Phi}{\alpha_c}\left[\frac{\alpha_t^{\,2}}{\left[1 + \left(\frac{\gamma - 1}{2}\right)\alpha_t^{\,2}\right]^{\frac{\gamma + 1}{\gamma - 1}}}\right]^{1/2} \qquad (A-4)$$

A-2

FIGURE A-1   SCHEMATIC REPRESENTATION OF THE VENT VALVE FOR
CALCULATION OF FLOW UNDER COMPRESSIBLE ADIABATIC
CONDITIONS

Using the definition of $\mathcal{P} = p/p_a$ and $\tau = t/t_{fill}$ in Eq. (13), and substituting Eq. (13) and (A-4) into the mass conservation equation $dM/dt = -\dot{M}_v$, we obtain:

$$\frac{d}{d\tau}[\mathcal{P}(1-\tau)] = -\frac{\mathcal{P}}{\alpha_c}\left[\frac{\alpha_t^2}{\left(1 + \frac{\gamma-1}{2}\alpha_t^2\right)^{\frac{\gamma+1}{\gamma-1}}}\right]^{1/2}$$

which is subject to the condition $\mathcal{P} = 1$ at $\tau = 0$.

Equations (A-1), (A-2), and (A-5) are three equations for the three unknowns α_t, α_e, and $\mathcal{P}$. α_t is determined for every value of $\mathcal{P}$ by solving simultaneously equations (A-1) and (A-2). That is, for a given exit pressure (which is generally the ambient tank pressure) and frictional coefficient, and guessing a value of tank pressure, we can solve equations (A-1) and (A-2) for α_t and α_e. This procedure is described in Appendix B. (Note when $\mathcal{P} = 1$, there is no flow, and therefore, α_t and $\alpha_e = 0$; of course, there is no friction either under these circumstances.)

As in the isothermal case, it simplifies the form of the equations to rewrite equation (A-5) as

$$\frac{d\mathcal{P}}{d\tau^1} = \mathcal{P} - \frac{\mathcal{P}}{\alpha_c}\left[\frac{\alpha_t^2}{\left[1 + \left(\frac{\gamma-1}{2}\right)\alpha_t^2\right]^{\frac{\gamma+1}{\gamma-1}}}\right]^{1/2} \qquad (A-6)$$

A-4

with $P = 1$ at $\tau^1 = 0$, where $\tau^1 = -\ell n \ (1-\tau)$; i.e., $\tau = 1-e^{-\tau^1}$.

The above equation has to be solved numerically.

A-5

Numerical Solution Procedure for Compressible Adiabatic Venting

In order to solve the governing Equation (A-1) and (A-2) set forth in Appendix A, let

$$
\left.
\begin{aligned}
\beta_t &= \frac{\gamma-1}{2}\, \alpha_t^{\,2} \\[2em]
\beta_e &= \frac{\gamma-1}{2}\, \alpha_e^{\,2}
\end{aligned}
\right\}
\tag{B-1}
$$

Then equations (A-1) and (A-2) become

$$
\frac{4\, f_e\, \gamma}{(\gamma-1)} = \left[\frac{1}{\beta_t} - \frac{1}{\beta_e}\right] + \left(\frac{\gamma+1}{\gamma-1}\right) \ln \frac{\beta_t\,(1+\beta_e)}{\beta_e\,(1+\beta_t)}
\tag{B-2}
$$

and

$$
\Phi = (1+\beta_t)^{\frac{\gamma}{\gamma-1}} \left[\frac{\beta_e\,(1+\beta_e)}{\beta_t\,(1+\beta_t)}\right]^{1/2}
$$

i.e.,

$$
\Phi = \left(\frac{\beta_e}{\beta_t}\right)(1+\beta_t)^{\frac{\gamma}{\gamma-1}} \left[\frac{\beta_t\,(1+\beta_e)}{\beta_e\,(1+\beta_t)}\right]^{1/2}
\tag{B-3}
$$

Hence, from (B-3) we get

$$
2\left[\ln \Phi - \ln \frac{\beta_e}{\beta_t}\,(1+\beta_t)^{\gamma/\gamma-1}\right] = \ln \frac{\beta_t\,(1+\beta_e)}{\beta_e\,(1+\beta_t)}
\tag{B-4}
$$

Substituting (B-4) in (B-2) we get

$$
(B-5)
$$

$$
\frac{4\,f_e\,\gamma}{(\gamma-1)} = \frac{1}{\beta_t}\left[1 - \frac{1}{(\beta_e/\beta_t)}\right] + \frac{2\,(\gamma+1)}{(\gamma-1)}\left\{\ln\Phi - \ln(\beta_e/\beta_t) - \frac{\gamma}{(\gamma-1)}\ln(1+\beta_t)\right\}
$$

Let $\qquad\qquad\qquad\qquad \beta_e/\beta_t = B$

Hence the two equations to be solved are

$$
\Phi = (1+\beta_t)^{\frac{\gamma}{\gamma-1}}\,B^{1/2}\left[\frac{1+\beta_e}{1+\beta_t}\right]^{1/2}
\qquad (B-6)
$$

$$
(B-7)
$$

$$
\left[\frac{4\,f_e\,\gamma}{(\gamma-1)} - \frac{2\,(\gamma+1)}{\gamma-1}\ln\Phi\right] = \frac{1}{\beta_t}\left[1 - \frac{1}{B}\right] - \frac{2\,(\gamma+1)}{(\gamma-1)}\left[\ln B + \frac{\gamma}{\gamma-1}\ln(1+\beta_t)\right]
$$

Eqs. (B-6) and (B-7) are two equations for two unknowns. Solve iteratively for one β in terms of the other until convergence is obtained.

APPENDIX C

Solution of the Governing Equation for Liquid Overfill

$$\frac{dp}{dt} = \frac{1}{(\beta + \kappa)} \left[\frac{(\dot{M}_i - \rho A U)}{M(o) + \dot{M}_i \, t - \int_o^t \rho A U \, dt} \right] \tag{C-1}$$

with

$$p = p_a + \rho g x + \frac{1}{2}(4f)\frac{y}{D}\rho U^2 \tag{C-2}$$

where

$$y = \int_o^t U \, dt \quad \text{for } y < L; \qquad y = L \, , \, y > L \tag{C-3}$$

$$x = y \text{ for } y < H$$
$$x = H \text{ for } y \geq H \tag{C-4}$$

We define the following characteristic and dimensionless parameters:

$$U_c = \frac{\dot{M}_i}{\rho A} \tag{C-5a}$$

$$v = U/U_c = \text{dimensionless outflow velocity} \tag{C-5b}$$

$$\overline{P} = \frac{(p - p_a)}{p_a} = \text{dimensionless gage pressure} \tag{C-5c}$$

$$P_D = \frac{\rho \, g \, D}{p_a} = \frac{\text{hydrostatic pressure due to a column of liquid}}{\text{equal to the diameter of vent pipe}} \tag{C-5d}$$

$$\lambda = \frac{\frac{1}{2}(4f)\rho \, U_c^2}{p_a} = \frac{\text{pressure drop due to flow at characteristic velo-}}{\text{city in a length of pipe equal to its diameter}} \tag{C-5e}$$

$$\xi = \frac{y}{L} \tag{C-5f}$$

$$t_c = \frac{L}{U_c} = \text{characteristic fill time for the vent pipe} \qquad\qquad \text{(C-5g)}$$

$$\tau = t/t_c = \text{dimensionless time} \qquad\qquad \text{(C-5h)}$$

$$H/L = \frac{\text{vertical length of vent pipe}}{\text{total length of vent pipe}} \qquad\qquad \text{(C-5i)}$$

$$\tau_{fill} = \frac{M(0)}{\dot{M}_i\, t_c} = \frac{\text{tank fill time}}{\text{characteristic vent fill time}} \qquad\qquad \text{(C-5j)}$$

Using the definitions in Equations C-5a through C-5j, we write Equation
(C-1) in dimensionless form as

$$\frac{dP}{d\tau} = \frac{1}{(\beta + \kappa)} \left[\frac{(1 - v)}{\tau_{fill} + \tau - \displaystyle\int_0^\tau v\, d\tau} \right] \qquad\qquad \text{(C-6)}$$

with $\overline{P} = 0$ at $\tau = 0$ \qquad\qquad (C-7)

$$\xi = \int_0^t v\, d\tau \qquad\qquad \text{(C-8)}$$

and from C-2, we have

$$\overline{P} = (L/D)_{pipe} [P_D + \lambda\, v^2]\, \xi \qquad \text{for } 0 < \xi \le H/L \qquad \text{(C-9a)}$$

$$\overline{P} = (L/D)_{pipe} [P_D\, H/L + \lambda\, \xi\, v^2] \qquad \text{for } H/L < \xi < 1 \qquad \text{(C-9b)}$$

$$\overline{P} = (L/D)_{pipe} [P_D\, H/L + \lambda\, v^2] + (L/D)_{valve}\, \lambda\, v^2 \qquad \text{after } \xi = 1 \qquad \text{(C-9c)}$$

Numerical procedure is used to solve for $\overline{P}$ and v as functions of time.
The details of the algorithm are given in Table C-1.

TABLE C-1

Sequence of Calculations to Solve Equations (C-6) and (C-9)

Time	Find	From Equation	Restriction
$\tau = 0$	v_o	$\dfrac{(1 - v_o)}{\tau_{fill}(\beta + \kappa)} = \left(\dfrac{L}{D}\right)_{pipe} (P_D v_o + \lambda v_o^3]$	$\xi < \xi_1$

(See Appendix D)

$$\xi_o = 0$$

$$\left(\frac{d\overline{P}}{d\tau}\right)_o = \frac{(1 - v_o)}{(\beta + \kappa)\tau_{fill}}$$

---

any τ
where
$\tau > 0$

$$\overline{P}_\tau = \overline{P}_{\tau - \Delta\tau} + \left(\frac{d\overline{P}}{d\tau}\right)_{\tau - \Delta\tau} \Delta\tau$$

If $\xi_{\tau - \Delta\tau} \leq \xi_1$

$$\xi_\tau = \frac{\overline{P}_\tau}{\left(\dfrac{L}{D}\right)_{pipe} [\overline{P}_D + \lambda v_{\tau - \Delta\tau}^2]}$$

$$v_\tau = \frac{2}{\Delta\tau} (\xi_\tau - \xi_{\tau - \Delta\tau}) - v_{\tau - \Delta\tau}$$

If $\xi_1 < \xi_{\tau - \Delta\tau} < 1$

$$v_\tau = \sqrt{[\overline{P}_{\tau - \Delta\tau} - \overline{P}_D (L/D) \xi_1]\bigg/ [(L/D) \lambda \xi_{\tau - \Delta\tau}]}$$

$$\xi_\tau = \xi_{\tau - \Delta\tau} + (v_\tau + v_{\tau - \Delta\tau}) \frac{\Delta\tau}{2}$$

If $\xi_{\tau - \Delta\tau} > 1$

$$\xi_\tau = 1$$

$$v_\tau = \left[(\overline{P}_\tau - \overline{P}_D \xi_1)\bigg/ \left(\left\{\frac{L}{D} + \left(\frac{L}{D}\right)_{valve}\right\} \lambda\right)\right]^{1/2}$$

$$\left(\frac{d\overline{P}}{d\tau}\right)_\tau = \frac{1 - v_\tau}{(\beta + \kappa) [\tau_{fill} + \tau - \xi_\tau]}$$

APPENDIX D

Evaluation of the Initial Liquid Overfill Velocity

Differentiating Equation C-9a with respect to τ, we have (using Eq. C-8),

$$\frac{d\overline{P}}{d\tau} = (L/D)_{pipe} \left\{ [P_D + \lambda\, v^2]\, v + (2\,\lambda \int_0^\tau v\, d\tau)\, v\, \frac{dv}{d\tau} \right\} \tag{D-1}$$

At $\tau = 0$, we have

$$\begin{array}{l} \text{Lim} \\ \tau \to 0 \end{array} \int_0^\tau v\, d\tau \to 0 \tag{D-2}$$

Also, from Equation C-6, we have

$$\frac{d\overline{P}}{d\tau} = \frac{1}{(\beta + \kappa)} \left[\frac{1 - v}{\tau_{fill} + \tau - \int_0^\tau v\, d\tau} \right] \tag{D-3}$$

Therefore, from Equations D-3 and D-1,

$$\begin{array}{l} \text{Lim} \\ \tau \to 0 \end{array} \frac{d\overline{P}}{d\tau} = \frac{1}{(\beta+\kappa)\tau_{fill}} \begin{array}{l} \text{Lim} \\ \tau \to 0 \end{array} (1 - v) = (L/D)_{pipe} \left[\begin{array}{l} \text{Lim} \\ \tau \to 0 \end{array} (P_D + \lambda\, v^2)v \right.$$

$$\left. + \begin{array}{l} \text{Lim} \\ \tau \to 0 \end{array} 2\,\lambda\, v\, \frac{dv}{d\tau} \int_0^\tau v\, d\tau \right] \tag{D-4}$$

There are three cases to consider for the above equation:

Case 1: $\begin{array}{l} \text{Lim} \\ \tau \to 0 \end{array} v = v_o = \text{finite}$

                    $\begin{array}{l} \text{Lim} \\ \tau \to 0 \end{array} \frac{dv}{d\tau} = \text{finite}$

D-1

Case 2:
$$\lim_{\tau \to 0} v = v_o = \text{finite}$$

$$\lim_{\tau \to 0} \frac{dv}{d\tau} = \text{infinite}$$

$$\lim_{\tau \to 0} \frac{dv}{d\tau} \int_o^\tau v \, d\tau \to \text{finite}$$

Case 3:
$$\lim_{\tau \to 0} v = 0$$

$$\lim_{\tau \to 0} \frac{dv}{d\tau} = \text{infinite}$$

$$\lim_{\tau \to 0} v \frac{dv}{d\tau} \int_o^\tau v \, d\tau = \text{finite}$$

Case 1: This is the simplest of the cases. Substituting $v = v_o$ in equation D-4, we get (in view of D-2)

$$\frac{(1 - v_o)}{(\beta + \kappa)\tau_{fill}} = (L/D)_{pipe} \ (P_D + \lambda v_o^2) \ v_o \qquad (D-5)$$

The above is a cubic equation in v_o. It can be shown that the equation has only one (positive) real solution. This can be obtained by using the exact method of solution for cubic equations (see Handbook of Mathematical Functions by M. Abramowitz and I. Stegun, page 7).

Case 2:

$$\text{Let } \xi = \int_0^\tau v \, d\tau \qquad \text{Therefore, } v = \frac{d\xi}{d\tau}$$

Now $\lim_{\tau \to 0} \xi \frac{dv}{d\tau} = \text{constant, say, } c$

with $\left(\frac{d\xi}{d\tau}\right)_{\tau \to 0} = v_{\tau \to 0} = \text{finite} = v_o$ and $\xi = 0$ at $\tau = 0$

Hence $\left(\xi \frac{dv}{dt}\right)_{\tau \to 0} = c$

i.e. $\left(\xi \frac{dv}{d\xi} \frac{d\xi}{d\tau}\right)_{\tau \to 0} = c$

i.e. $\left(\xi \dfrac{dv}{d\xi}\right)_{\tau \to 0} v_o = c$

i.e. $\left[\dfrac{dv}{d\ln\xi}\right]_{\tau \to 0} = (c/v_o)$

Let us approach $\tau \to 0$ on the line.

$$\frac{dv}{d\ln\xi} = (c/v_o)$$

Therefore, $v = c/v_o \, \ln\xi$ + constant of integration

However, from the boundary condition,

$v = v_o$ at $\xi = 0$

This cannot be satisfied by the above equation. Hence, Case 2 is not a possible case.

Case 3: By an analysis similar to that shown in Case 2, it can be shown that this is also a physically _invalid_ case. Hence, the only possible solution to Equation D-4 is given by the solution of the cubic Equation D-5.

Hence, $U_o = v_o \times U_c$ (D-6)

APPENDIX E

Volume Expansion Due to Deflection
of Bulkhead Panels and Stiffeners

Objective

In the analysis of the cargo overfill problem, it was found that as the tank pressure began to build up due to the flow resistance in the vent system, the tank walls expand. The value of the linear expansion parameter, $\beta = (1/V) \, dV/dP$, which is the fractional volume change per unit pressure change, is very important to the analysis and is estimated as follows:

Approach

Assuming there is no cargo in the adjacent tanks to counteract the lateral pressure loadings on the bulkhead, we envision two deflections which can be analyzed by structural formulae:

- Deflection of panels; and

- Deflection of stiffners.
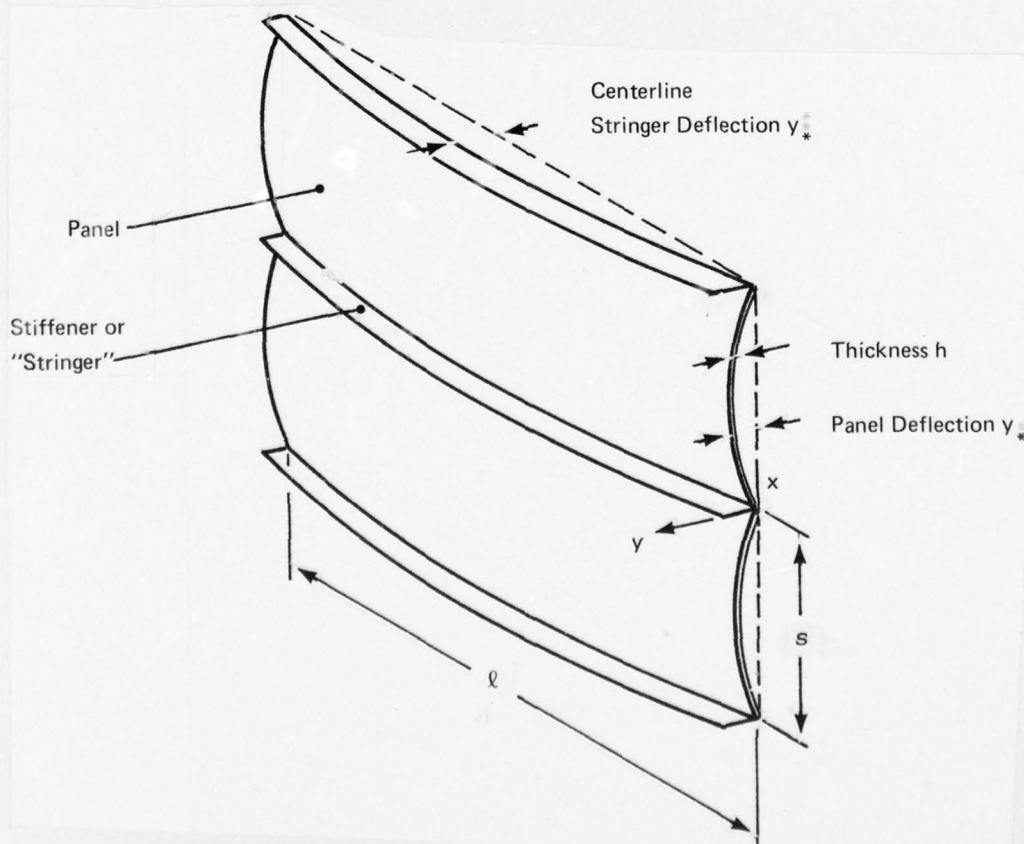
This situation is pictured below in Figure E-1.

FIGURE E-1   BULKHEAD SECTION UNDERGOING DEFLECTION

E-1

First we must derive an expression for the volume change ΔV as a function of the centerline deflection y_*, which depends on the contour of the deflection and the geometry of the panel. In addition, we can use structural formulas for y_* as a function of the pressure. Mathematically, we write the two relationships we seek as follows:

$$V = V_T + \Delta V\ (y_*) \tag{E-1}$$

$$y_* = f\ (P) \tag{E-2}$$

Once we have these relationships, we can substitute (E-2) into (E-1) and differentiate with respect to pressure to obtain the expansion parameter

$$\beta = \frac{1}{V_T} \frac{dV}{dP} \tag{E-3}$$

Volume Change as a Function of Centerline Deflection

We take the panels as two dimensional since they are usually long rectangles. In general, ΔV for an array of N two-dimensional panels fixed on both edges can be expressed as an integral over the panel width coordinate x:

$$\Delta V = N\ell \int_o^b y\,dx = N\ell s \int_o^1 y\,d\eta, \tag{E-4}$$

where $\eta = x/s$ and the configuration is shown in Figure E-1.

We will apply Equation (E-4) to both elastic and plastic deflection cases.

Now for an <u>elastic</u> uniformly loaded panel, we have[*]

$$y = y_* \bigg|_{\text{elastic}} 16 \, \eta^2 \, (1 - 2\eta + \eta^2).$$ (E-5)

This defines the contour along the deflected edge. Substituting (E-5) into (E-4) we obtain

$$\Delta V_{\text{elastic}} = Ns\ell \, y_* \bigg|_{\text{elastic}} 16 \int_0^1 (\eta^2 - 2\eta^3 + \eta^4) \, d\eta$$

which gives

$$\Delta V_{\text{elastic}} = \frac{8}{15} \, Ns\ell \, y_* \bigg|_{\text{elastic}}$$ (E-6)

For a <u>plastic</u> uniformly loaded panel, the contour equation is given by[*]

$$y = y_* \bigg|_{\text{plastic}} \frac{16}{5} \, \eta \, (1 - 2\eta^3 + \eta^3).$$ (E-7)

Substituting (E-7) into (E-4) we obtain

$$\Delta V_{\text{plastic}} = Ns\ell \, y_* \bigg|_{\text{plastic}} \cdot \frac{16}{5} \int_0^1 (\eta - 2\eta^3 + \eta^4) \, d\eta$$

---

[*] Bleish, <u>Formulas for Stress and Strain</u>.

which gives

$$\Delta V_{\text{plastic}} = \frac{16}{25} \, Ns \, \ell \, y_{*_{\text{plastic}}} \tag{E-8}$$

Centerline Deflection as a Function of Pressure

For the plastic and elastic cases we have the following expressions for a uniformly loaded plate:

$$y_{*_{\text{elastic}}} = \frac{1}{24} \, \frac{W}{EI} \left(\frac{s^3}{16} \right)$$

$$y_{*_{\text{plastic}}} = \frac{1}{24} \, \frac{W}{EI} \left(\frac{5s^3}{16} \right)$$

where W = Load in pounds

E = Modulus of elasticity, and

I = Moment of inertia of panel or beam section = $h^3 \ell / 12$.

Note that $y_{*_{\text{plastic}}}$ is five times $y_{*_{\text{elastic}}}$.

Now the pressure $P = W/s\ell$ so we have

$$y_{*_{\text{elastic}}} = \frac{1}{24} \, \frac{P\ell}{EI} \, \frac{s^4}{16} \tag{E-9}$$

$$y_{*_{\text{plastic}}} = \frac{1}{24} \, \frac{P\ell}{EI} \, \frac{5s^4}{16} \tag{E-10}$$

Calculation of Expansion Parameter B

Substituting (E-9) into (E-6) and (E-10) into (E-8) we obtain

$$\Delta V_{\text{plastic}} = \frac{1}{120} \, \frac{N\ell s^5 P}{EI} \tag{E-11}$$

and
$$\Delta V_{elastic} = \frac{1}{720} \frac{N \ell s^5 P}{EI} \qquad (E-12)$$

Employing Equation (E-3) we obtain

$$\beta_{plastic} = \frac{N s^5 \ell^2}{120 V_T EI} \qquad (E-13)$$

$$\beta_{elastic} = \frac{N s^5 \ell^2}{720 V_T EI} \qquad (E-14)$$

where V_T is the normal tank volume and N is the number of panels.

Substituting typical values for a tank having four hundred 9 x 3 ft panels we obtain

$\ell = 9$ ft
$V_T = 7 \times 10^4$ ft^3
$N = 400$
$s = 3$ ft
$E = 2.9 \times 10^7$ psi
$I = 9.3$ in^4 (thickness h = 1.0 inch)

We obtain for plastic deflection (E-13) of <u>panels</u> only:

$$\beta = .74 \times 10^{-4} \ (psi)^{-1}$$

This is equivalent to a total volume added of 100 ft^3 at the point of incident failure (20 psig), which is approximately 1/7% of the normal tank volume.

A similar analysis for <u>stiffeners</u> was carried out, and a value of β was obtained approximately equal to the above value for <u>panels</u>. Therefore, the volume expansion coefficient is estimated to be approximately

$$\beta \simeq .0001 \ psi^{-1}$$

for a typical vessel. For any particular vessel, the value of β could range from .001 to .00001 depending on the number of panels, panel dimensions, and stiffener spacing.